PHYSICAL REVIEW E **79**, 031109 (2009)

Field theory of bicritical and tetracritical points. III. Relaxational dynamics including conservation of magnetization (model C)

R. Folk,[1,*] Yu. Holovatch,[2,1,†] and G. Moser[3,‡]

[1]Institute for Theoretical Physics, Johannes Kepler University Linz, Altenbergerstrasse 69, A-4040, Linz, Austria

[2]Institute for Condensed Matter Physics, National Academy of Sciences of Ukraine, 1 Svientsitskii Street, UA-79011 Lviv, Ukraine

[3]Department for Material Research and Physics, Paris Lodron University Salzburg, Hellbrunnerstrasse 34, A-5020 Salzburg, Austria

(Received 1 December 2008; published 12 March 2009)

We calculate the relaxational dynamical critical behavior of systems of $O(n_\|)\oplus O(n_\perp)$ symmetry including conservation of magnetization by renormalization group theory within the minimal subtraction scheme in two-loop order. Within the stability region of the Heisenberg fixed point and the biconical fixed point, strong dynamical scaling holds, with the asymptotic dynamical critical exponent $z=2\phi/\nu-1$, where ϕ is the crossover exponent and ν the exponent of the correlation length. The critical dynamics at $n_\|=1$ and $n_\perp=2$ is governed by a small dynamical transient exponent leading to nonuniversal nonasymptotic dynamical behavior. This may be seen, e.g., in the temperature dependence of the magnetic transport coefficients.

DOI: 10.1103/PhysRevE.79.031109 PACS number(s): 05.50.+q, 64.60.Ht

I. INTRODUCTION

In two previous papers [1,2] (referred to as paper I and paper II henceforth) we have considered the critical statics and relaxational dynamics of $O(n_\|)\oplus O(n_\perp)$ physical systems near the multicritical point where the two phase transition lines of the system corresponding to $O(n_\|)$ and $O(n_\perp)$ symmetry meet. The space of the order parameter (OP) dimensions $n_\|$ and $n_\perp$ decomposes in regions where the multicritical behavior is described by different fixed points (FPs)—the $O(n=n_\|+n_\perp)$ isotropic FP, the biconical FP, and the decoupling FP—and a region where no stable FP is found (runaway region) (see Fig. 1 in paper I). In the resummed two-loop-order field theoretic treatment it was found that for integer values of $n_\|$ and $n_\perp$ the biconical FP is stable only for a system with $n_\|=1$, $n_\perp=2$, and its symmetric counterpart. For specific initial conditions of the nonuniversal parameters of the system the $O(n=n_\|+n_\perp)$ isotropic FP (Heisenberg FP) might also be reached. Such a system is physically represented by an antiferromagnet in an external magnetic field. The two cases mentioned above correspond to tetracritical and bicritical multicritical points, respectively. If no FP is reached the multicritical point might be of first order, i.e., a triple point.

The dynamics of the antiferromagnet in a magnetic field is quite complicated and the equations of motion have been formulated for slow densities by Dohm and Janssen [3]. These equations contain reversible and irreversible coupling terms between the OPs (the components of the staggered magnetization parallel and perpendicular to the magnetic field) and one conserved density (the parallel component of the magnetization). In fact there is a second conserved density (CD)—the energy density—which in general should be taken into account, but it will not be included here since in two-loop order the specific heat exponent at the biconical FP turned out to be negative [4] for the case $n_\|=1$ and $n_\perp=2$. Concerning the new static results [1], a simplified dynamical model [3] has been reconsidered [2], consisting of two relaxational equations for the two OPs. The time scale ratio v between the two relaxation rates $\Gamma_\|$ and $\Gamma_\perp$ introduces a very small dynamical transient since the dynamical FP lies very near to the stability boundary separating strong and weak dynamical scaling. The strong dynamical scaling FP is governed by $v^\star$ finite and different from zero whereas the weak dynamical scaling FP by $v^\star=0$ or ∞.

A further step to the complete model is to include the diffusive dynamics of the slow CD, leading to a model-C-like extension. In this extended model a new time scale ratio appears, defined by the ratio of one of the OP relaxation rates to the kinetic coefficient λ of the conserved density m. This model has been studied in one-loop order in Refs. [3,5,6] taking into account only some of the dynamical two-loop-order terms and one-loop statics. Here we present a complete two-loop-order calculations.

The inclusion of further densities in addition to the OP makes it necessary to extend the static functional of the usual ϕ^4 theory, although the OP alone would be sufficient to describe the static critical behavior. Such an extended static functional for isotropic systems [$O(n)$ symmetry] with short-range interaction has the form [7,8]

$$\mathcal{H}^{(C)}=\int d^dx\left(\frac{1}{2}\mathring{\tilde{r}}\vec{\phi}_0\cdot\vec{\phi}_0+\frac{1}{2}\sum_{i=1}^{n}\nabla_i\vec{\phi}_0\cdot\nabla_i\vec{\phi}_0+\frac{1}{2}m_0^2+\frac{\mathring{\tilde{u}}}{4!}(\vec{\phi}_0\cdot\vec{\phi}_0)^2+\frac{1}{2}\mathring{\gamma}m_0\vec{\phi}_0\cdot\vec{\phi}_0-\mathring{h}m_0\right). \qquad (1)$$

Here the order parameter $\vec{\phi}_0\equiv\vec{\phi}_0(x)$ is assumed to be an n-component real vector, and the symbol $\cdot$ denotes the scalar product. The secondary density $m_0\equiv m_0(x)$ is considered as a scalar quantity and $\mathring{h}$ is the field conjugated to m_0. It is chosen to have a vanishing average value $\langle m_0\rangle=0$. Within stat-

*folk@tphys.uni-linz.ac.at

†hol@icmp.lviv.ua

‡guenter.moser@sbg.ac.at

ics, the above functional is equivalent to the Ginzburg-Landau-Wilson (GLW) functional

$$\mathcal{H}_{\rm GLW} = \int d^dx \Bigg(\frac{1}{2}\mathring{r}\vec{\phi}_0 \cdot \vec{\phi}_0 + \frac{1}{2}\sum_{i=1}^{n} \nabla_i\vec{\phi}_0 \cdot \nabla_i\vec{\phi}_0 + \frac{\mathring{u}}{4!}(\vec{\phi}_0 \cdot \vec{\phi}_0)^2 \Bigg), \tag{2}$$

where $\mathring{r}$ is proportional to the temperature distance to the critical point and $\mathring{u}$ is the fourth-order coupling in which perturbation expansion is usually performed. The GLW functional (2) is obtained by integrating out the CD, which appears only in Gaussian order in (1), in the corresponding partition function. The parameters $\mathring{\tilde{r}}$, $\mathring{\tilde{u}}$, and $\mathring{\gamma}$ in (1) and $\mathring{r}$ and $\mathring{u}$ in (2) are related by

$$\mathring{r} = \mathring{\tilde{r}} + \mathring{\gamma}\mathring{h}, \quad \mathring{u} = \mathring{\tilde{u}} - 3\mathring{\gamma}^2. \tag{3}$$

The extended static functional appears in the driving force of the equations of motion for the OP $\vec{\phi}_0$ and the CD m_0. The ratio of the kinetic coefficient $\mathring{\Gamma}$ in the relaxation equation for the OP and the kinetic coefficient $\mathring{\lambda}$ in the diffusive equation for the CD defines the dynamical parameter w whose FP value governs the dynamical scaling of the model.

It is worthwhile to summarize some results for model C at a usual critical point, where the CD can be identified with an energylike density and the value of the specific heat exponent α (in any case) governs the relevance of the asymmetric static coupling $\mathring{\gamma}$ between the OP and the CD. Namely, this coupling is irrelevant in the renormalization group (RG) sense—it vanishes at the FP—if the specific heat exponent is negative, i.e., the specific heat of the system does not diverge at the critical point. If the specific heat diverges then there remain two possibilities for the dynamical FP: either the FP value of the ratio w between the time scale of the OP and that of the CD is different from zero and finite, or it is zero or infinite. In the first case strong dynamical scaling with one time scale for the OP and the CD is realized with one dynamical scaling exponent $z=2+\alpha/\nu$ (ν is the exponent of the correlation length). In the second case weak dynamical scaling is present and the time scale of the OP is different from the time scale of the CD, both represented by a corresponding dynamical critical exponent. This region of the weak dynamical scaling FP is tiny (see, e.g., Fig. 1 in Ref. [8]). One should note that at the usual critical point an asymmetric coupling to the OP as given in Eq. (1) is always "energylike" independent of its physical origin. That means the divergence of the CD susceptibility is always described by the specific heat exponent α.

In the case of a multicritical point treated here the situation is more complicated since there are two OPs and a CD might couple to both of these OPs. As has been shown in paper I after a proper rotation [Eq. (64)] in the OP space temperature- and magneticlike field directions can be identified. In consequence at the multicritical point one has to discriminate the cases of energy and magnetization conservation.

The paper is organized as follows. In Sec. II we extend model C of the O(n)-symmetrical critical system to the case of an $O(n_\|)\oplus O(n_\perp)$ symmetrical multicritical point as considered in papers I and II. The renormalization is performed in Sec. III and the field theoretic functions are calculated in Sec. IV. Then we discuss the possible FPs and their stability in Sec. V. The effective dynamical critical behavior is considered in Sec. VI, followed in Sec. VII by a short summary of the results and an outlook on further work to be done.

II. MODEL C FOR MULTICRITICAL POINTS

A. Static functional

In order to describe the multicritical behavior the n-dimensional space of the order parameter components is split into two subspaces with dimensions $n_\perp$ and $n_\|$ with the property $n_\perp + n_\| = n$. The order parameter separates into

$$\vec{\phi}_0 = \begin{pmatrix} \vec{\phi}_{\perp 0} \\ \vec{\phi}_{\| 0} \end{pmatrix}, \tag{4}$$

where $\vec{\phi}_{\perp 0}$ is the $n_\perp$-dimensional order parameter of the $n_\perp$ subspace, and $\vec{\phi}_{\| 0}$ is the $n_\|$-dimensional order parameter of the $n_\|$ subspace. Introducing this separation into the GLW functional (2) one obtains

$$\mathcal{H}_{Bi} = \int d^dx \Bigg(\frac{1}{2}\mathring{r}_\perp \vec{\phi}_{\perp 0} \cdot \vec{\phi}_{\perp 0} + \frac{1}{2}\sum_{i=1}^{n_\perp} \nabla_i\vec{\phi}_{\perp 0} \cdot \nabla_i\vec{\phi}_{\perp 0} + \frac{1}{2}\mathring{r}_\| \vec{\phi}_{\| 0} \cdot \vec{\phi}_{\| 0} + \frac{1}{2}\sum_{i=1}^{n_\|} \nabla_i\vec{\phi}_{\| 0} \cdot \nabla_i\vec{\phi}_{\| 0} + \frac{\mathring{u}_\perp}{4!}(\vec{\phi}_{\perp 0} \cdot \vec{\phi}_{\perp 0})^2 + \frac{\mathring{u}_\|}{4!}(\vec{\phi}_{\| 0} \cdot \vec{\phi}_{\| 0})^2 + \frac{2\mathring{u}_\times}{4!}(\vec{\phi}_{\perp 0} \cdot \vec{\phi}_{\perp 0})(\vec{\phi}_{\| 0} \cdot \vec{\phi}_{\| 0}) \Bigg), \tag{5}$$

which represents a multicritical Ginzburg-Landau-Wilson model. The properties of this functional concerning renormalization, regions of stable FPs, and corresponding type of multicritical behavior were extensively discussed in paper I (see [9] for earlier references). The separation (4) has now to be performed in (1). The resulting functional is

$$\mathcal{H}_{Bi}^{(C)} = \int d^dx \Bigg(\frac{1}{2}\mathring{\tilde{r}}_\perp \vec{\phi}_{\perp 0} \cdot \vec{\phi}_{\perp 0} + \frac{1}{2}\sum_{i=1}^{n_\perp} \nabla_i\vec{\phi}_{\perp 0} \cdot \nabla_i\vec{\phi}_{\perp 0} + \frac{1}{2}\mathring{\tilde{r}}_\| \vec{\phi}_{\| 0} \cdot \vec{\phi}_{\| 0} + \frac{1}{2}\sum_{i=1}^{n_\|} \nabla_i\vec{\phi}_{\| 0} \cdot \nabla_i\vec{\phi}_{\| 0} + \frac{1}{2}m_0^2 + \frac{\mathring{\tilde{u}}_\perp}{4!}(\vec{\phi}_{\perp 0} \cdot \vec{\phi}_{\perp 0})^2 + \frac{\mathring{\tilde{u}}_\|}{4!}(\vec{\phi}_{\| 0} \cdot \vec{\phi}_{\| 0})^2 + \frac{2\mathring{\tilde{u}}_\times}{4!}(\vec{\phi}_{\perp 0} \cdot \vec{\phi}_{\perp 0})(\vec{\phi}_{\| 0} \cdot \vec{\phi}_{\| 0}) + \frac{1}{2}\mathring{\gamma}_\perp m_0 \vec{\phi}_{\perp 0} \cdot \vec{\phi}_{\perp 0} + \frac{1}{2}\mathring{\gamma}_\| m_0 \vec{\phi}_{\| 0} \cdot \vec{\phi}_{\| 0} - \mathring{h} m_0 \Bigg). \tag{6}$$

By integrating the contributions of the secondary density in the corresponding partition function, (6) reduces to the static functional (5). Relations analogous to (3) between the parameters of the two static functionals arise. They read

$$\mathring{r}_\perp = \mathring{\tilde{r}}_\perp + \mathring{\gamma}_\perp \mathring{h}, \quad \mathring{u}_\perp = \mathring{\tilde{u}}_\perp - 3\mathring{\gamma}_\perp^2, \tag{7}$$

$$\mathring{r}_\parallel = \mathring{\tilde{r}}_\parallel + \mathring{\gamma}_\parallel \mathring{h}, \quad \mathring{u}_\parallel = \mathring{\tilde{u}}_\parallel - 3\mathring{\gamma}_\parallel^2, \tag{8}$$

$$\mathring{u}_\times = \mathring{\tilde{u}}_\times - 3\mathring{\gamma}_\perp \mathring{\gamma}_\parallel. \tag{9}$$

Because the partition function calculated from (6) is reducible to a partition function based on (5) by integration, the correlation functions, or vertex functions, respectively, of the secondary density m_0 are exactly related to correlation functions of the order parameter. This leads to several relations that are important for the renormalization. In particular, the average value of m_0 and the two-point correlation function are defined as

$$\langle m_0\rangle \equiv \frac{1}{\mathcal{N}_{Bi}^{(C)}}\int \mathcal{D}(\phi_{\perp 0},\phi_{\parallel 0},m_0)m_0 e^{-\mathcal{H}_{Bi}^{(C)}}, \tag{10}$$

$$\langle m_0 m_0\rangle \equiv \frac{1}{\mathcal{N}_{Bi}^{(C)}}\int \mathcal{D}(\phi_{\perp 0},\phi_{\parallel 0},m_0)m_0 m_0 e^{-\mathcal{H}_{Bi}^{(C)}}, \tag{11}$$

with $\mathcal{N}_{Bi}^{(C)}=\int\mathcal{D}(\phi_{\perp 0},\phi_{\parallel 0},m_0)e^{-\mathcal{H}_{Bi}^{(C)}}$ as the normalization constant and $\mathcal{D}(\phi_{\perp 0},\phi_{\parallel 0},m_0)$ as a suitable integral measure. Performing the integration over m_0 in (10) and using Eqs. (7)–(9), the average value of m_0 reads

$$\langle m_0\rangle = \mathring{h} - \mathring{\gamma}_\perp\left\langle \frac{1}{2}\vec{\phi}_{\perp 0}^2\right\rangle - \mathring{\gamma}_\parallel\left\langle \frac{1}{2}\vec{\phi}_{\parallel 0}^2\right\rangle, \tag{12}$$

where $\vec{\phi}^2$ denotes quadratic insertions of the order parameter. Their average values on the right-hand side of (12),

$$\left\langle \frac{1}{2}\vec{\phi}_{\alpha_i 0}^2\right\rangle = \frac{1}{\mathcal{N}_{Bi}}\int \mathcal{D}(\phi_{\perp 0},\phi_{\parallel 0})\frac{1}{2}\vec{\phi}_{\alpha_i 0}^2 e^{-\mathcal{H}_{Bi}}, \tag{13}$$

are now calculated with the static functional (5) and $\mathcal{N}_{Bi}=\int\mathcal{D}(\phi_{\perp 0},\phi_{\parallel 0})e^{-\mathcal{H}_{Bi}}$. In order to obtain $\langle m_0\rangle=0$ the conjugated external field is chosen as

$$\mathring{h} = \mathring{\gamma}_\perp\left\langle \frac{1}{2}\vec{\phi}_{\perp 0}^2\right\rangle + \mathring{\gamma}_\parallel\left\langle \frac{1}{2}\vec{\phi}_{\parallel 0}^2\right\rangle. \tag{14}$$

Quite analogously, by integrating m_0 in (11) one obtains the following relation for the two-point correlation function of the secondary density:

$$\langle m_0 m_0\rangle_c = 1 - \mathring{\boldsymbol{\gamma}}^T\cdot\mathring{\boldsymbol{\Gamma}}^{(0,2)}\cdot\mathring{\boldsymbol{\gamma}}. \tag{15}$$

In (15) we have introduced the column matrix

$$\mathring{\boldsymbol{\gamma}} \equiv \begin{pmatrix}\mathring{\gamma}_\perp\\ \mathring{\gamma}_\parallel\end{pmatrix}. \tag{16}$$

The superscript T indicates a transposed vector or matrix, while the subscript c on the average at the left-hand side of (15) denotes the cumulant $\langle AB\rangle_c\equiv\langle AB\rangle-\langle A\rangle\langle B\rangle$. The matrix

$$\mathring{\boldsymbol{\Gamma}}^{(0,2)} = \begin{pmatrix}\mathring{\Gamma}^{(0,2)}_{;\perp\perp} & \mathring{\Gamma}^{(0,2)}_{;\perp\parallel}\\ \mathring{\Gamma}^{(0,2)}_{;\parallel\perp} & \mathring{\Gamma}^{(0,2)}_{;\parallel\parallel}\end{pmatrix} = -\begin{pmatrix}\left\langle \frac{1}{2}\vec{\phi}_{\perp 0}^2\frac{1}{2}\vec{\phi}_{\perp 0}^2\right\rangle_c & \left\langle \frac{1}{2}\vec{\phi}_{\perp 0}^2\frac{1}{2}\vec{\phi}_{\parallel 0}^2\right\rangle_c\\ \left\langle \frac{1}{2}\vec{\phi}_{\perp 0}^2\frac{1}{2}\vec{\phi}_{\parallel 0}^2\right\rangle_c & \left\langle \frac{1}{2}\vec{\phi}_{\parallel 0}^2\frac{1}{2}\vec{\phi}_{\parallel 0}^2\right\rangle_c\end{pmatrix} \tag{17}$$

of two-point vertex functions is related to correlations of ϕ^2 insertions. The vertex functions generally were introduced in paper I (Sec. III), and in particular the matrix (17) (renormalized counterpart) in Eq. (83) therein. A third important relation can be obtained by differentiating the average value (10) by $\mathring{\tilde{h}}$ at fixed parameters $\Delta\mathring{\tilde{r}}_\alpha$, $\mathring{\tilde{u}}_\alpha$, $\mathring{\gamma}_\alpha$. In $\Delta\mathring{\tilde{r}}_\alpha=\mathring{\tilde{r}}_\alpha-\mathring{\tilde{r}}_{\alpha_i c}$ the shift of the critical temperature has been taken into account (for more details, see Appendix 1 in paper I). As a result one obtains

$$\left.\frac{\partial}{\partial\mathring{h}}\langle m_0(x)\rangle\right|_{\Delta\mathring{\tilde{r}}_\alpha,\mathring{\tilde{u}}_\alpha,\mathring{\gamma}_\alpha} = \int dx'\langle m_0(x)m_0(x')\rangle_c. \tag{18}$$

From relation (14) the external field is a function of $\Delta\mathring{r}_\alpha$. The h derivative in (18) can be rewritten as $\Delta\mathring{r}_\alpha$ derivatives. Finally one obtains

$$\int dx'\langle m_0(x)m_0(x')\rangle_c = \left.\mathring{\boldsymbol{\gamma}}^T\cdot\frac{\partial}{\partial\Delta\mathring{\boldsymbol{r}}}\langle m_0(x)\rangle\right|_{\Delta\mathring{\tilde{r}}_\alpha,\mathring{\tilde{u}}_\alpha,\mathring{\gamma}_\alpha} \tag{19}$$

where we have defined

$$\frac{\partial}{\partial\Delta\mathring{\boldsymbol{r}}} \equiv \begin{pmatrix}\partial/\partial\Delta\mathring{r}_\perp\\ \partial/\partial\Delta\mathring{r}_\parallel\end{pmatrix}. \tag{20}$$

All static vertex functions, for the order parameter as well as for the secondary density, may be calculated with (6) in a perturbation expansion as functions of the correlation lengths $\{\xi\}\equiv\{\xi_\perp,\xi_\parallel\}$, the set of quartic couplings $\{\mathring{\tilde{u}}\}\equiv\{\mathring{\tilde{u}}_\perp,\mathring{\tilde{u}}_\parallel,\mathring{\tilde{u}}_\times\}$, the set of asymmetric couplings $\{\mathring{\gamma}\}\equiv\{\mathring{\gamma}_\perp,\mathring{\gamma}_\parallel\}$, and the wave vector modulus k. The parameters in the order parameter vertex functions $\mathring{\tilde{\Gamma}}^{(N,L)}_{\alpha_1\cdots\alpha_N;i_1\cdots i_L}$ (for the notation see Appendix 1 in paper I) via relations (7)–(9) combine the corresponding parameters of the multicritical GLW model (5). Thus all order parameter vertex functions calculated with (6) have the property

$$\mathring{\tilde{\Gamma}}^{(N,L)}_{\alpha_1\cdots\alpha_N;i_1\cdots i_L}(\{\xi\},k,\{\mathring{\tilde{u}}\},\{\mathring{\gamma}\}) = \mathring{\Gamma}^{(N,L)}_{\alpha_1\cdots\alpha_N;i_1\cdots i_L}(\{\xi\},k,\{\mathring{u}\}), \tag{21}$$

meaning that they are identical to corresponding functions of the multicritical GLW model (5). For this reason no distinction between the correlation lengths entering the left- and right-hand sides of (21) is necessary. The correlation lengths are defined from the two-point order parameter vertex functions at the left side with (6), and on the right side with (5) [see Eqs. (A7) and (A8) in paper I]. Vertex functions of the secondary density can be expressed as functions of $\{\mathring{u}\}$ instead of $\{\mathring{\tilde{u}}\}$ by using (7)–(9). In particular, the two-point function $\mathring{\bar{\Gamma}}_{mm}=\langle m_0 m_0\rangle_c^{-1}$, which will be of interest in the following, can be written as

$$\mathring{\bar{\Gamma}}_{mm}(\{\xi\},k,\{\mathring{\tilde{u}}\},\{\mathring{\gamma}\}) = \mathring{\Gamma}_{mm}(\{\xi\},k,\{\mathring{u}\},\{\mathring{\gamma}\}). \tag{22}$$

B. Dynamical model

The dynamical equations of model A in paper II have now to be extended by appending a diffusion equation for the secondary density. One obtains

$$\frac{\partial \vec{\phi}_{\perp 0}}{\partial t} = -\mathring{\Gamma}_{\perp}\frac{\delta \mathcal{H}_{Bi}^{(C)}}{\delta \vec{\phi}_{\perp 0}} + \vec{\theta}_{\phi_{\perp}}, \tag{23}$$

$$\frac{\partial \vec{\phi}_{\parallel 0}}{\partial t} = -\mathring{\Gamma}_{\parallel}\frac{\delta \mathcal{H}_{Bi}^{(C)}}{\delta \vec{\phi}_{\parallel 0}} + \vec{\theta}_{\phi_{\parallel}}, \tag{24}$$

$$\frac{\partial m_0}{\partial t} = \mathring{\lambda}\nabla^2\frac{\delta \mathcal{H}_{Bi}^{(C)}}{\delta m_0} + \theta_m. \tag{25}$$

In addition to the two kinetic coefficients $\mathring{\Gamma}_{\perp}$ and $\mathring{\Gamma}_{\parallel}$ of the order parameter in the corresponding subspaces, a kinetic coefficient $\mathring{\lambda}$ of diffusive type for the conserved secondary density is now present. The stochastic forces $\vec{\theta}_{\phi_{\perp}}$, $\vec{\theta}_{\phi_{\parallel}}$, and θ_m satisfy the Einstein relations

$$\langle \theta_{\phi_{\perp}}^{\alpha}(x,t)\theta_{\phi_{\perp}}^{\beta}(x',t')\rangle = 2\mathring{\Gamma}_{\perp}\delta(x-x')\delta(t-t')\delta^{\alpha\beta}, \tag{26}$$

$$\langle \theta_{\phi_{\parallel}}^{i}(x,t)\theta_{\phi_{\parallel}}^{j}(x',t')\rangle = 2\mathring{\Gamma}_{\parallel}\delta(x-x')\delta(t-t')\delta^{ij}, \tag{27}$$

$$\langle \theta_m(x,t)\theta_m(x',t')\rangle = -2\mathring{\lambda}\nabla^2\delta(x-x')\delta(t-t'), \tag{28}$$

with indices $\alpha,\beta=1,\ldots,n_{\perp}$ and $i,j=1,\ldots,n_{\parallel}$ corresponding to the two subspaces. The dynamical two-point vertex function of the secondary density has a general structure quite analogous to the corresponding functions of the order parameter [see Eqs. (6) and (7) in paper II]. One can write

$$\mathring{\Gamma}_{m\tilde{m}}(\{\xi\},k,\omega) = -i\omega\mathring{\Omega}_{m\tilde{m}}(\{\xi\},k,\omega) + \mathring{\Gamma}_{mm}(\{\xi\},k)\mathring{\lambda}k^2, \tag{29}$$

where $\mathring{\Gamma}_{mm}(\{\xi\},k)$ is the static two-point function discussed in the previous section and $\mathring{\Omega}_{m\tilde{m}}(\{\xi\},k,\omega)$ is a genuine dynamical function [8]. $\tilde{m}$ is the auxiliary density corresponding to m. For brevity, we have dropped the couplings and kinetic coefficients in the argument lists of (29).

III. RENORMALIZATION

A. Renormalization of the static parameters

As a consequence of the discussion at the end of Sec. II A all vertex functions will be expanded in powers of the quartic couplings $\{\mathring{u}\}$ of the multicritical GLW model and the asymmetric couplings $\{\mathring{\gamma}\}$. The renormalization scheme introduced in Sec. III in paper I remains valid and will be used in the following. The corresponding definitions and relations can be found therein and will not be repeated here. In particular, we implement the minimal subtraction RG scheme directly at $d=3$ [10,11] to two-loop order. In the current extended model additional renormalizations for the secondary density m_0 and the asymmetric couplings $\{\mathring{\gamma}\}$ have to be considered. The renormalized counterparts of the secondary density and the asymmetric couplings are introduced as

$$m_0 = Z_m m, \tag{30}$$

$$\mathring{\vec{\gamma}} = \kappa^{\varepsilon/2}Z_m^{-1}\boldsymbol{Z}_{\phi}^{-1}\cdot\boldsymbol{Z}_{\gamma}\cdot\vec{\gamma}A_d^{-1/2}, \tag{31}$$

where κ is the usual reference wave vector modulus and $\varepsilon=4-d$. The geometrical factor A_d and the diagonal matrix $\boldsymbol{Z}_{\phi}$ were defined in Eqs. (8) and (17) of paper I. With (30) and (31) at hand, the renormalization for the CD two-point vertex function Γ_{mm} readily follows:

$$\Gamma_{mm} = Z_m^2\mathring{\Gamma}_{mm}. \tag{32}$$

The additional Z factor Z_m and the matrix $\boldsymbol{Z}_{\gamma}$ are related to the known renormalization factors of the multicritical GLW model as a consequence of the reducibility of the extended model to the multicritical GLW model.

From the condition that (19) is also valid for the renormalized counterparts of the appearing quantities the relation

$$\boldsymbol{Z}_{\gamma} = Z_m^2\boldsymbol{Z}_r = Z_m^2\boldsymbol{Z}_{\phi}\cdot\boldsymbol{Z}_{\phi^2}^T \tag{33}$$

follows. For the second equality, relation (18) of paper I has been used. The Z factors of the asymmetric couplings are determined by the renormalizations of the secondary density and the ϕ^2 insertions in the multicritical GLW model.

Relation (15) establishes a connection between the correlation functions of the CD and the ϕ^2 insertions in the multicritical GLW model. This relation should be invariant under renormalization. Thus the renormalization of the secondary density is related by

$$Z_m^{-2} = 1 + \vec{\gamma}^T\cdot\boldsymbol{A}(\{u\})\cdot\vec{\gamma} \tag{34}$$

to the additive renormalization $\boldsymbol{A}(\{u\})$ of the correlation function of the ϕ^2 insertions (17) in the multicritical GLW model introduced in Eq. (15) in paper I.

B. Renormalization of the dynamical parameters

The general form of the renormalization of the auxiliary densities $\tilde{\vec{\phi}}_{\perp 0}$ and $\tilde{\vec{\phi}}_{\parallel 0}$ and the kinetic coefficients $\mathring{\Gamma}_{\perp}$ and $\mathring{\Gamma}_{\parallel}$ has been presented within model A in Sec. III A in paper II. It remains valid and will be used in the following. Of course, new contributions occur to the dynamical renormalization factors especially of the kinetic coefficients

$$\mathring{\Gamma}_{\perp} = Z_{\Gamma_{\perp}}\Gamma_{\perp}, \quad \mathring{\Gamma}_{\parallel} = Z_{\Gamma_{\parallel}}\Gamma_{\parallel}, \tag{35}$$

due to the asymmetric coupling $\vec{\gamma}$.

Within model C additional renormalizations are necessary only for the auxiliary density $\tilde{m}_0$ and the kinetic coefficient $\mathring{\lambda}$. Thus we introduce

$$\tilde{m}_0 = Z_{\tilde{m}}\tilde{m}, \quad \mathring{\lambda} = Z_\lambda \lambda. \tag{36}$$

In the case of conserved densities the dynamical function $\mathring{\Omega}_{m\tilde{m}}(\{\xi\},k,\omega)$ in (29) does not contain new dimensional singularities. Therefore the corresponding auxiliary density $\tilde{m}_0$ needs no independent renormalization. The Z factor $Z_{\tilde{m}}$ is determined by the relation

$$Z_{\tilde{m}} = Z_m^{-1}. \tag{37}$$

Due to the absence of mode coupling terms, the renormalization of the kinetic coefficient λ is completely determined by the static renormalization and Z_λ is

$$Z_\lambda = Z_m^2. \tag{38}$$

IV. ζ AND β FUNCTIONS

As already mentioned in the preceding section, the renormalization of the GLW functional remains valid. This validates also all ζ and β functions introduced in Sec. IV in paper I. We do not repeat them here, although they will be used in the following.

A. Static functions

Apart from the three β functions $\beta_{u_\perp}$, $\beta_{u_\times}$, and $\beta_{u_\parallel}$ and the two ζ matrices $\boldsymbol{B}_{\phi^2}$ and $\boldsymbol{\zeta}_{\phi^2}$ appearing in the multicritical GLW model (see Sec. IV in paper I), an additional ζ function ζ_m and a column matrix of β functions for the asymmetric coupling (16) have to be introduced. The relations between the renormalization factors discussed in Sec. III A give rise to corresponding relations between the ζ and β functions. It follows immediately from (34),

$$\zeta_m(\{u\},\{\gamma\}) \equiv \frac{d \ln Z_m^{-1}}{d \ln \kappa} = \frac{1}{2}\vec{\gamma}^T \cdot \boldsymbol{B}_{\phi^2}(\{u\}) \cdot \vec{\gamma}, \tag{39}$$

where $\boldsymbol{B}_{\phi^2}(\{u\})$ has been defined in Eq. (30) in paper I. The κ derivatives also in the following definitions always are taken at fixed unrenormalized parameters. Inserting the two-loop expression of $\boldsymbol{B}_{\phi^2}(\{u\})$ [see Eq. (31) in paper I] we obtain

$$\zeta_m(\{u\},\{\gamma\}) = \frac{n_\perp}{4}\gamma_\perp^2 + \frac{n_\parallel}{4}\gamma_\parallel^2. \tag{40}$$

The column matrix of the β functions for the asymmetric coupling $\vec{\gamma}$ is defined as

$$\vec{\beta}_\gamma(\{u\},\{\gamma\}) \equiv \kappa \frac{d\vec{\gamma}}{d\kappa}. \tag{41}$$

Inserting Eq. (31) into the above definition, one obtains together with relation (33) the expression

$$\vec{\beta}_\gamma(\{u\},\{\gamma\}) = \left[\left(-\frac{\varepsilon}{2} + \zeta_m\right)\mathbf{1} + \boldsymbol{\zeta}_{\phi^2}^T(\{u\})\right] \cdot \vec{\gamma}. \tag{42}$$

There $\mathbf{1}$ denotes the two-dimensional unit matrix. The matrix $\boldsymbol{\zeta}_{\phi^2}(\{u\})$ was introduced in paper I [see Eq. (22)]. The ζ function ζ_m is exactly known from (39). Thus finally we arrive at

$$\vec{\beta}_\gamma(\{u\},\{\gamma\}) = \left[\left(-\frac{\varepsilon}{2} + \frac{1}{2}\vec{\gamma}^T \cdot \boldsymbol{B}_{\phi^2}(\{u\}) \cdot \vec{\gamma}\right)\mathbf{1} + \boldsymbol{\zeta}_{\phi^2}^T(\{u\})\right] \cdot \vec{\gamma}. \tag{43}$$

The above expression is valid in all orders of perturbation expansion. $\boldsymbol{B}_{\phi^2}(\{u\})$ and $\boldsymbol{\zeta}_{\phi^2}(\{u\})$ are calculated in loop expansion within the multicritical GLW model. Their-two loop expressions were given in Eqs. (31) and (23)–(26) in paper I.

B. Dynamical functions

Using relation (38), the ζ function ζ_λ corresponding to the kinetic coefficient λ is simply given by

$$\zeta_\lambda(\{u\},\{\gamma\}) \equiv \frac{d \ln Z_\lambda^{-1}}{d \ln \kappa} = 2\zeta_m(\{u\},\{\gamma\}). \tag{44}$$

The dynamical ζ functions of the kinetic coefficients of the order parameter are defined by

$$\zeta_{\Gamma_\alpha}^{(C)}(\{u\},\{\gamma\},\{w\}) \equiv \frac{d \ln Z_{\Gamma_\alpha}^{-1}}{d \ln \kappa}, \quad \alpha = \parallel, \perp. \tag{45}$$

In the model C dynamics, they get nontrivial contributions from the asymmetric couplings $\gamma_\perp$ and $\gamma_\parallel$. They read now in two-loop order

$$\begin{aligned}\zeta_{\Gamma_\perp}^{(C)}(\{u\},\{\gamma\},\{w\}) = {}& \bar{\zeta}^{(C_\perp)}(u_\perp,\gamma_\perp,w_\perp) \\ & - \frac{n_\parallel}{4}\frac{w_\perp\gamma_\perp\gamma_\parallel}{1+w_\perp}\left(\frac{2}{3}u_\times + \frac{w_\perp\gamma_\perp\gamma_\parallel}{1+w_\perp}\right) \\ & \times\left[1 + \ln\frac{2v}{1+v} - \left(1+\frac{2}{v}\right)\ln\frac{2(1+v)}{2+v}\right] \\ & + \zeta_{\Gamma_\perp}^{(A)}(u_\perp,u_\times,v),\end{aligned} \tag{46}$$

$$\begin{aligned}\zeta_{\Gamma_\parallel}^{(C)}(\{u\},\{\gamma\},\{w\}) = {}& \bar{\zeta}^{(C_\parallel)}(u_\parallel,\gamma_\parallel,w_\parallel) \\ & - \frac{n_\perp}{4}\frac{w_\parallel\gamma_\parallel\gamma_\perp}{1+w_\parallel}\left(\frac{2}{3}u_\times + \frac{w_\parallel\gamma_\parallel\gamma_\perp}{1+w_\parallel}\right) \\ & \times\left(1 + \ln\frac{2}{1+v} - (1+2v)\ln\frac{2(1+v)}{1+2v}\right) \\ & + \zeta_{\Gamma_\parallel}^{(A)}(u_\parallel,u_\times,v),\end{aligned} \tag{47}$$

where we have defined the time scale ratios

$$w_\perp = \frac{\Gamma_\perp}{\lambda}, \quad w_\parallel = \frac{\Gamma_\parallel}{\lambda}. \tag{48}$$

The ratio v is defined as in paper II as the ratio

$$v \equiv \frac{\Gamma_\parallel}{\Gamma_\perp} = \frac{w_\parallel}{w_\perp}, \tag{49}$$

and is therefore a function of $w_\perp$ and $w_\parallel$. In (46) and (47) several ζ functions of known subsystems have already been introduced. $\zeta_{\Gamma_\alpha}^{(A)}(u_\alpha,u_\times,v)$ with $\alpha=\|$ or $\perp$ are the ζ functions of the full multicritical model A presented explicitly in paper II [see Eqs. (14) and (15) therein],

$$\zeta_{\Gamma_\perp}^{(A)} = \frac{n_\perp+2}{36}u_\perp^2\left(3\ln\frac{4}{3}-\frac{1}{2}\right) + \frac{n_\|}{36}u_\times^2\left(\frac{2}{v}\ln\frac{2(1+v)}{2+v}+\ln\frac{(1+v)^2}{v(2+v)}-\frac{1}{2}\right), \quad (50)$$

$$\zeta_{\Gamma_\|}^{(A)} = \frac{n_\|+2}{36}u_\|^2\left(3\ln\frac{4}{3}-\frac{1}{2}\right) + \frac{n_\perp}{36}u_\times^2\left(2v\ln\frac{2(1+v)}{1+2v}+\ln\frac{(1+v)^2}{1+2v}-\frac{1}{2}\right), \quad (51)$$

where $\bar{\zeta}^{(C_\alpha)}(u,\gamma,w)$ are the genuine ζ functions of model C within the n_α-component subspaces without pure fourth-order coupling terms (pure model A terms). They were given explicitly in [12] for an n-component system in two-loop order. These contributions of model C in the n-component subspaces without the corresponding model A terms are [8]

$$\bar{\zeta}_{\Gamma_\|}^{(C_\alpha)}(u,\gamma,w) = \frac{w\gamma^2}{1+w}\left\{1-\frac{1}{2}\left[\frac{n_\alpha+2}{3}u\left(1-3\ln\frac{4}{3}\right) + \frac{w\gamma^2}{1+w}\left(\frac{n_\alpha}{2}-\frac{w}{1+w}-\frac{3(n_\alpha+2)}{2}\ln\frac{4}{3} - \frac{(1+2w)}{1+w}\ln\frac{(1+w)^2}{1+2w}\right)\right]\right\}. \quad (52)$$

The β functions corresponding to the time scale ratios (48) and (49) can be expressed in terms of the corresponding ζ functions of the kinetic coefficients:

$$\beta_v \equiv \kappa\frac{dv}{d\kappa} = v(\zeta_{\Gamma_\|}^{(C)}-\zeta_{\Gamma_\perp}^{(C)}), \quad (53)$$

$$\beta_{w_\|} \equiv \kappa\frac{dw_\|}{d\kappa} = w_\|(\zeta_{\Gamma_\|}^{(C)}-\zeta_\lambda), \quad (54)$$

$$\beta_{w_\perp} \equiv \kappa\frac{dw_\perp}{d\kappa} = w_\perp(\zeta_{\Gamma_\perp}^{(C)}-\zeta_\lambda), \quad (55)$$

with the κ derivatives taken at fixed unrenormalized parameters.

Note that these equations are not independent but one of the three equations can be eliminated by the relation $v(l)=w_\|(l)/w_\perp(l)$, which of course holds also for the initial conditions.

V. FIXED POINTS AND THEIR STABILITY

A. Static fixed points

The FPs of the couplings u_a and their stability were studied in Sec. V of paper I. Their values and the corresponding transient exponents were listed in Table I there. Let us recall that, depending on the values of $n_\|$ and $n_\perp$, one of the following FPs is stable and governs multicritical behavior: the isotropic Heisenberg FP $\mathcal{H}(n_\|+n_\perp)$ with $u_\|^\star=u_\perp^\star=u_\times^\star\neq 0$, the decoupling FP $\mathcal{D}$ with $u_\|^\star\neq 0$, $u_\perp^\star\neq 0$, and $u_\times^\star=0$, and the biconical FP with nonequal $u_\|^\star\neq 0$, $u_\perp^\star\neq 0$, and $u_\times^\star\neq 0$. For each of the FPs of paper I one can now determine the FP values for $\gamma_\perp$ and $\gamma_\|$ from the equation

$$\vec{\beta}_\gamma(\{u^\star\},\{\gamma^\star\}) = \left[\left(-\frac{\varepsilon}{2}+\frac{1}{2}\vec{\gamma}^{\star T}\cdot \boldsymbol{B}_{\phi^2}(\{u^\star\})\cdot\vec{\gamma}^\star\right)\mathbf{1} + \boldsymbol{\zeta}_{\phi^2}^T(\{u^\star\})\right]\cdot\vec{\gamma}^\star = 0. \quad (56)$$

This splits each FP of paper I into a set of FPs in the combined $\{u\}$-$\{\gamma\}$ space, which are equivalent in statics but different in dynamics. Note that Eq. (56) includes two equations that have to be solved for given FP values of the quartic couplings $\{u^\star\}$. The static FPs of paper I can be roughly separated into three classes: (i) the Gaussian FP $\mathcal{G}$, with $u_a^\star=0$ for all couplings; (ii) the decoupling FPs $\mathcal{H}(n_\perp)$, $\mathcal{H}(n_\|)$, and $\mathcal{D}$, where $u_\times^\star=0$; (iii) the isotropic Heisenberg and biconical FPs $\mathcal{H}(n_\perp+n_\|)$ and $\mathcal{B}$ where all $u_a^\star$ are different from zero. We list the FP values of the corresponding asymmetric couplings $\gamma_\|^\star$ and $\gamma_\perp^\star$ in Table I, which summarizes our analysis given below. Note that $\gamma_\perp^\star=0$, $\gamma_\|^\star=0$ is of course always a solution of Eq. (56), independent of the values of $\{u^\star\}$. We do not list this trivial solution explicitly in Table I, although this may be the stable FP for definite values of $n_\perp$ and $n_\|$ in some cases.

1. Gaussian fixed point $\mathcal{G}$

At this FP one has $\boldsymbol{\zeta}_{\phi^2}=\mathbf{0}$ and the two equations in (56) reduce to the condition

$$\frac{n_\perp}{2}\gamma_\perp^{\star 2}+\frac{n_\|}{2}\gamma_\|^{\star 2}=\varepsilon, \quad (57)$$

which is valid in all orders of perturbation expansion. The above equation defines a line of FPs.

2. Heisenberg and decoupling fixed points $\mathcal{H}(n_\perp)$, $\mathcal{H}(n_\|)$, and $\mathcal{D}$

At these FPs, where the cross coupling $u_\times$ vanishes, the matrix $\boldsymbol{\zeta}_{\phi^2}$ has the form

$$\boldsymbol{\zeta}_{\phi^2}(u_\times=0) = \begin{pmatrix} \zeta_{\phi^2}^{(n_\perp)}(u_\perp) & 0 \\ 0 & \zeta_{\phi^2}^{(n_\|)}(u_\|) \end{pmatrix}. \quad (58)$$

The function $\zeta_{\phi^2}^{(n_\alpha)}(u_\alpha)$ is the well-known ζ function of the n_α-component isotropic system. Equation (56) reduces to

$$\left(-\frac{\varepsilon}{2}+\frac{1}{2}\vec{\gamma}^{\star T}\cdot\boldsymbol{B}_{\phi^2}(\{u^\star\})\cdot\vec{\gamma}^\star+\zeta_{\phi^2}^{(n_\perp)}(u_\perp^\star)\right)\gamma_\perp=0, \quad (59)$$

$$\left(-\frac{\varepsilon}{2}+\frac{1}{2}\vec{\gamma}^{\star T}\cdot\boldsymbol{B}_{\phi^2}(\{u^\star\})\cdot\vec{\gamma}^\star+\zeta_{\phi^2}^{(n_\|)}(u_\|^\star)\right)\gamma_\|=0, \quad (60)$$

where the matrix $\boldsymbol{B}_{\phi^2}$ is of the form

TABLE I. Fixed points of the asymmetric couplings $\gamma_\perp$ and $\gamma_\parallel$ of the extended $O(n_\parallel)\oplus O(n_\perp)$ model. The values of the isotropic Heisenberg FP $\mathcal{H}(n_\perp+n_\parallel)$ and the biconical FP $\mathcal{B}$ are valid in two-loop order because Eq. (75) has been used. For all other FPs the expressions are valid in all orders of perturbation expansion.

FP	$\gamma_\perp^\star/\gamma_\parallel^\star$	$\gamma_\perp^{\star 2}$	$\gamma_\parallel^{\star 2}$
$\mathcal{G}$	Line of FPs (57)	Line of FPs (57)	Line of FPs (57)
$\mathcal{H}(n_\perp)$	0	0	$\frac{2}{n_\parallel}\varepsilon$
	∞	$\frac{\varepsilon-2\zeta_{\phi^2}^{(n_\perp)}(u_\perp^\star)}{B_{\phi^2}^{(n_\perp)}(u_\perp^\star)}$	0
$\mathcal{H}(n_\parallel)$	∞	$\frac{2}{n_\perp}\varepsilon$	0
	0	0	$\frac{\varepsilon-2\zeta_{\phi^2}^{(n_\parallel)}(u_\parallel^\star)}{B_{\phi^2}^{(n_\parallel)}(u_\parallel^\star)}$
$\mathcal{D}$	∞	$\frac{\varepsilon-2\zeta_{\phi^2}^{(n_\perp)}(u_\perp^\star)}{B_{\phi^2}^{(n_\perp)}(u_\perp^\star)}$	0
	0	0	$\frac{\varepsilon-2\zeta_{\phi^2}^{(n_\parallel)}(u_\parallel^\star)}{B_{\phi^2}^{(n_\parallel)}(u_\parallel^\star)}$
$\mathcal{H}(n_\perp+n_\parallel)$, $\mathcal{B}$	$\frac{\zeta_+^\star-[\boldsymbol{\zeta}_{\phi^2}^\star]_{22}}{[\boldsymbol{\zeta}_{\phi^2}^\star]_{12}}$	$\frac{2(\varepsilon-2\zeta_+^\star)}{n_\perp+n_\parallel\left(\frac{[\boldsymbol{\zeta}_{\phi^2}^\star]_{12}}{\zeta_+^\star-[\boldsymbol{\zeta}_{\phi^2}^\star]_{22}}\right)^2}$	$\frac{2(\varepsilon-2\zeta_+^\star)}{n_\perp\left(\frac{\zeta_+^\star-[\boldsymbol{\zeta}_{\phi^2}^\star]_{22}}{[\boldsymbol{\zeta}_{\phi^2}^\star]_{12}}\right)^2+n_\parallel}$
	$\frac{[\boldsymbol{\zeta}_{\phi^2}^\star]_{21}}{\zeta_-^\star-[\boldsymbol{\zeta}_{\phi^2}^\star]_{11}}$	$\frac{2(\varepsilon-2\zeta_-^\star)}{n_\perp+n_\parallel\left(\frac{\zeta_-^\star-[\boldsymbol{\zeta}_{\phi^2}^\star]_{11}}{[\boldsymbol{\zeta}_{\phi^2}^\star]_{21}}\right)^2}$	$\frac{2(\varepsilon-2\zeta_-^\star)}{n_\perp\left(\frac{[\boldsymbol{\zeta}_{\phi^2}^\star]_{21}}{\zeta_-^\star-[\boldsymbol{\zeta}_{\phi^2}^\star]_{11}}\right)^2+n_\parallel}$

$$\boldsymbol{B}_{\phi^2}(u_\times=0)=\begin{pmatrix} B_{\phi^2}^{(n_\perp)}(u_\perp) & 0 \\ 0 & B_{\phi^2}^{(n_\parallel)}(u_\parallel)\end{pmatrix}. \tag{61}$$

The nontrivial FP values for $\gamma_\perp$ and $\gamma_\parallel$ resulting from Eqs. (59) and (60) are listed in Table I. They are valid in all orders of perturbation expansion.

We want to remark that in Table I only FPs that exist for arbitrary order parameter component numbers are given. For special n values a line of FPs exists where both asymmetric couplings γ_α are different from zero. In the case $n_\perp=n_\parallel=n/2$, one has $u_\perp^\star=u_\parallel^\star=\bar{u}^\star$ and the ζ functions in Eqs. (59) and (60) are equal, leading to $\gamma_\perp^{\star 2}+\gamma_\parallel^{\star 2}=[\varepsilon-2\zeta_{\phi^2}^{(n/2)}(\bar{u}^\star)]/B_{\phi^2}^{(n/2)}(\bar{u}^\star)$.

3. Isotropic Heisenberg and biconical FPs $\mathcal{H}(n_\perp+n_\parallel)$ and $\mathcal{B}$

At the isotropic Heisenberg FP $\mathcal{H}(n_\perp+n_\parallel)$ and the biconical FP $\mathcal{B}$, where all couplings u_a are different from zero, it is more convenient to transform the matrix $\boldsymbol{\zeta}_{\phi^2}$ into its diagonal form with the transformation

$$\begin{pmatrix} \zeta_+ & 0 \\ 0 & \zeta_- \end{pmatrix}=\boldsymbol{P}^{-1}\cdot\boldsymbol{\zeta}_{\phi^2}^T\cdot\boldsymbol{P} \tag{62}$$

introduced in Sec. VI B in paper I. Inserting (62) into Eq. (56) leads to the transformed β function

$$\vec{\beta}_\gamma=\boldsymbol{P}\cdot\vec{\beta}_{\gamma_\pm} \tag{63}$$

with

$$\vec{\beta}_{\gamma_\pm}=\left[\left(-\frac{\varepsilon}{2}+\frac{1}{2}\vec{\gamma}^T\cdot\boldsymbol{B}_{\phi^2}\cdot\vec{\gamma}\right)\mathbf{1}+\begin{pmatrix} \zeta_+ & 0 \\ 0 & \zeta_- \end{pmatrix}\right]\cdot\vec{\gamma}_\pm. \tag{64}$$

Here, the transformed asymmetric coupling column matrix is defined as

$$\vec{\gamma}_\pm\equiv\begin{pmatrix}\gamma_+ \\ \gamma_-\end{pmatrix}=\boldsymbol{P}^{-1}\cdot\vec{\gamma}. \tag{65}$$

Note that the scalar quantity

$$\vec{\gamma}^T \cdot \boldsymbol{B}_{\phi^2} \cdot \vec{\gamma} = \vec{\gamma}_{\pm}^T \cdot \boldsymbol{B}_{\phi^2}^{(\pm)} \cdot \vec{\gamma}_{\pm}, \tag{66}$$

where $\boldsymbol{B}_{\phi^2}^{(\pm)} = \boldsymbol{P}^T \cdot \boldsymbol{B}_{\phi^2} \cdot \boldsymbol{P}$, is invariant under transformation. Therefore in (64) it is written in the untransformed form. At the FP Eq. (63) reduces to the condition

$$\vec{\beta}_{\gamma_{\pm}}(\{u^\star\},\{\gamma^\star\}) = 0, \tag{67}$$

because the determinant of matrix $\boldsymbol{P}$ does not vanish. Subsequently, Eq. (64) leads to two FP equations

$$(-\varepsilon + \vec{\gamma}^{\star T} \cdot \boldsymbol{B}_{\phi^2}^\star \cdot \vec{\gamma}^\star + 2\zeta_+^\star)\gamma_+^\star = 0, \tag{68}$$

$$(-\varepsilon + \vec{\gamma}^{\star T} \cdot \boldsymbol{B}_{\phi^2}^\star \cdot \vec{\gamma}^\star + 2\zeta_-^\star)\gamma_-^\star = 0. \tag{69}$$

In the above equations we have introduced the shorthand notations $\boldsymbol{B}_{\phi^2}^\star \equiv \boldsymbol{B}_{\phi^2}(\{u^\star\})$ and $\zeta_{\pm}^\star \equiv \zeta_{\pm}(\{u^\star\})$. If both transformed asymmetric couplings $\gamma_+^\star$ and $\gamma_-^\star$ are different from zero, the above two equations lead to the condition $\zeta_+^\star = \zeta_-^\star$. This condition is not valid if *all* quartic couplings $u_a^\star$ are different from zero. Thus at least one of the two transformed asymmetric couplings, γ_+ or γ_-, has to be zero at the FP. The transformation matrix $\boldsymbol{P}$ has been presented in Eq. (64) in paper I. Expressed in terms of the ζ functions, it reads

$$\boldsymbol{P} = \begin{pmatrix} P_{11} & P_{12} \\ P_{21} & P_{22} \end{pmatrix} = \begin{pmatrix} 1 & \dfrac{[\boldsymbol{\zeta}_{\phi^2}]_{21}}{\zeta_- - [\boldsymbol{\zeta}_{\phi^2}]_{11}} \\ \dfrac{[\boldsymbol{\zeta}_{\phi^2}]_{12}}{\zeta_+ - [\boldsymbol{\zeta}_{\phi^2}]_{22}} & 1 \end{pmatrix}, \tag{70}$$

where $[\boldsymbol{\zeta}_{\phi^2}]_{ij}$ are the elements of the matrix $\boldsymbol{\zeta}_{\phi^2}$ [for the two-loop expressions see Eqs. (23)–(26) in paper I].

Let us now consider the two cases where one of the asymmetric couplings is nonzero.

Case (a): $\gamma_+^\star \neq 0$, $\gamma_-^\star = 0$. Taking into account Eq. (65) the condition for a vanishing $\gamma_-^\star$ reads $-P_{21}\gamma_\perp^\star + P_{11}\gamma_\parallel^\star = 0$. Given the matrix elements (70) it can be rewritten as

$$\frac{\gamma_\parallel^\star}{\gamma_\perp^\star} = \frac{[\boldsymbol{\zeta}_{\phi^2}^\star]_{12}}{\zeta_+^\star - [\boldsymbol{\zeta}_{\phi^2}^\star]_{22}}. \tag{71}$$

At finite $\gamma_+^\star$ the expression in parentheses in Eq. (68) has to vanish, which results in the condition

$$2\zeta_m^\star = \vec{\gamma}^{\star T} \cdot \boldsymbol{B}_{\phi^2}^\star \cdot \vec{\gamma}^\star = \varepsilon - 2\zeta_+^\star = \frac{\alpha}{\nu}. \tag{72}$$

The last equality uses the definition of the asymptotic exponents derived in paper I [Eq. (90) there].

Case (b): $\gamma_+^\star = 0$, $\gamma_-^\star \neq 0$. In this case Eq. (65) leads immediately to the condition $P_{22}\gamma_\perp^\star - P_{12}\gamma_\parallel^\star = 0$. Inserting (70) gives

$$\frac{\gamma_\perp^\star}{\gamma_\parallel^\star} = \frac{[\boldsymbol{\zeta}_{\phi^2}^\star]_{21}}{\zeta_-^\star - [\boldsymbol{\zeta}_{\phi^2}^\star]_{11}}. \tag{73}$$

At finite $\gamma_-^\star$ the expression in parentheses in Eq. (69) has to vanish, which results in the condition

$$2\zeta_m^\star = \vec{\gamma}^{\star T} \cdot \boldsymbol{B}_{\phi^2}^\star \cdot \vec{\gamma}^\star = \varepsilon - 2\zeta_-^\star = 2\frac{\phi}{\nu} - d. \tag{74}$$

Again, the last equality uses the definition of the asymptotic exponents derived in paper I [Eq. (82) there], where ϕ is the crossover exponent. The above equations (71)–(74), respectively, determine the FP values of the two asymmetric couplings in the corresponding cases. The relations are valid in all orders of perturbation expansion.

Since in two-loop order $\boldsymbol{B}_{\phi^2}^\star$ is diagonal and independent of the couplings $\{u\}$ [see Eq. (31) in paper I] the left-hand sides of Eqs. (72) and (74) read

$$\vec{\gamma}^{\star T} \cdot \boldsymbol{B}_{\phi^2}^\star \cdot \vec{\gamma}^\star = \gamma_\perp^{\star 2}\frac{n_\perp}{2} + \gamma_\parallel^{\star 2}\frac{n_\parallel}{2}. \tag{75}$$

In consequence the asymmetric static couplings are zero when the exponent expressions on the right-hand sides of (72) and (74) are zero. This is the case if the energy-like CD and/or the magnetzation-like CD susceptibility do not diverge.

Using (75) together with (71)–(74) leads to the FP values of the asymmetric couplings $\gamma_\parallel^{\star 2}$ and $\gamma_\perp^{\star 2}$.

Case (a): $\gamma_+^\star \neq 0$, $\gamma_-^\star = 0$:

$$\gamma_\perp^{\star 2} = \frac{2(\varepsilon - 2\zeta_+^\star)}{n_\perp + n_\parallel\left(\dfrac{[\boldsymbol{\zeta}_{\phi^2}^\star]_{12}}{\zeta_+^\star - [\boldsymbol{\zeta}_{\phi^2}^\star]_{22}}\right)^2}, \tag{76}$$

$$\gamma_\parallel^{\star 2} = \frac{2(\varepsilon - 2\zeta_+^\star)}{n_\perp\left(\dfrac{\zeta_+^\star - [\boldsymbol{\zeta}_{\phi^2}^\star]_{22}}{[\boldsymbol{\zeta}_{\phi^2}^\star]_{12}}\right)^2 + n_\parallel}. \tag{77}$$

Case (b): $\gamma_+^\star = 0$, $\gamma_-^\star \neq 0$:

$$\gamma_\perp^{\star 2} = \frac{2(\varepsilon - 2\zeta_-^\star)}{n_\perp + n_\parallel\left(\dfrac{\zeta_-^\star - [\boldsymbol{\zeta}_{\phi^2}^\star]_{11}}{[\boldsymbol{\zeta}_{\phi^2}^\star]_{21}}\right)^2}, \tag{78}$$

$$\gamma_\parallel^{\star 2} = \frac{2(\varepsilon - 2\zeta_-^\star)}{n_\perp\left(\dfrac{[\boldsymbol{\zeta}_{\phi^2}^\star]_{21}}{\zeta_-^\star - [\boldsymbol{\zeta}_{\phi^2}^\star]_{11}}\right)^2 + n_\parallel}. \tag{79}$$

Note that the ratios in (71) and (73) might be negative, leading to a negative product $\gamma_\parallel^\star\gamma_\perp^\star$.

The explicit values of the above FPs depend on whether the isotropic Heisenberg or the biconical FP is inserted into the ζ functions. Equations (76)–(79) are valid up to two-loop order. In three-loop order it is known from the isotropic GLW model that the function B_{ϕ^2} gets u^2 contributions [13]. In the multicritical GLW model the matrix $\boldsymbol{B}_{\phi^2}$ may also be nondiagonal, and then Eq. (75) does not hold in this simple form.

In the case of the *isotropic Heisenberg FP* $u_\perp^\star = u_\parallel^\star = u_\times^\star = u^\star$, Eqs. (76)–(79) simplify considerably. The ratios of the elements of the $\boldsymbol{\zeta}_{\phi^2}$ matrix reduce to

$$\frac{[\zeta^{\star}_{\phi^2}]_{12}}{\zeta^{\star}_{+}-[\zeta^{\star}_{\phi^2}]_{22}}=1=\frac{\gamma^{\star}_{\parallel}}{\gamma^{\star}_{\perp}} \tag{80}$$

for case (a) and

$$\frac{[\zeta^{\star}_{\phi^2}]_{21}}{\zeta^{\star}_{-}-[\zeta^{\star}_{\phi^2}]_{11}}=-\frac{n_{\parallel}}{n_{\perp}}=\frac{\gamma^{\star}_{\perp}}{\gamma^{\star}_{\parallel}} \tag{81}$$

for case (b). For the second equalities (71) and (73) have been used. Together with the relations $\varepsilon-2\zeta^{\star}_{+}=\alpha/\nu$ and $\varepsilon-2\zeta^{\star}_{-}=\phi/\nu-d$, which introduce the critical exponents and follow from Eqs. (80)–(82) in paper I, the values for the isotropic Heisenberg FP are as follows.

Case (a): $\gamma^{\star}_{+}\neq 0$, $\gamma^{\star}_{-}=0$:

$$\gamma^{\star 2}_{\perp}=\gamma^{\star 2}_{\parallel}=\frac{2}{n_{\perp}+n_{\parallel}}\frac{\alpha}{\nu}. \tag{82}$$

Case (b): $\gamma^{\star}_{+}=0$, $\gamma^{\star}_{-}\neq 0$:

$$\gamma^{\star 2}_{\perp}=\frac{2}{n_{\perp}+n_{\parallel}}\frac{n_{\parallel}}{n_{\perp}}\left(2\frac{\phi}{\nu}-d\right), \tag{83}$$

$$\gamma^{\star 2}_{\parallel}=\frac{2}{n_{\perp}+n_{\parallel}}\frac{n_{\perp}}{n_{\parallel}}\left(2\frac{\phi}{\nu}-d\right). \tag{84}$$

Note that due to the sign in Eq. (81) the relation

$$\gamma^{\star}_{\parallel}\gamma^{\star}_{\perp}=-\frac{2}{n_{\perp}+n_{\parallel}}\left(2\frac{\phi}{\nu}-d\right) \tag{85}$$

holds in this case. For $n_{\parallel}=1$ and $n_{\perp}=2$ our results agree with those of Ref. [6].

4. Resummation procedure

As in our previous papers [1,2] of this series, in order to get numerical estimates we proceed within the fixed dimension RG technique, i.e., we evaluate RG expansions in couplings $\{u_{\parallel},u_{\perp},u_{\times}\}$ at fixed $d=3$. Furthermore, as long as the expansions are known to have zero radius of convergence, we use the resummation technique [14] to get reliable numerical estimates. The results given below were obtained within such a technique applied to the two-loop RG expansions. One of the ways to judge the typical numerical accuracy of our data is to give an estimate for some cases where the expansions (and, consequently, their numerical estimates) are known within a much higher order of loops. Since the static exponents α and ν explicitly enter many of the formulas considered above, let us take them as an example. Namely, let us estimate the relations

$$(2\phi/\nu-d)|_{d=3}\equiv 2/\nu_{-}-3, \tag{86}$$

$$\alpha/\nu|_{d=3}\equiv 2/\nu_{+}-3 \tag{87}$$

that enter the formulas for the couplings $\gamma_{\perp}$ and $\gamma_{\parallel}$. The exponents ν_{+} and ν_{-} were defined in Eqs. (80) and (81) of paper I. Figure 1 shows the dependence of $2\phi/\nu-3$ and of α/ν on the order parameter component numbers $n_{\perp}$ at fixed $n_{\parallel}=1$. Recall that of main interest for us will be the physical case $n_{\parallel}=1$, $n_{\perp}=2$ indicated by the arrow. The region of $n_{\perp}$ shown in the figure contains also the region of stability of the Heisenberg O(n)-symmetrical FP, with $n=n_{\parallel}+n_{\perp}$. In particular, it starts near the marginal field dimension n_c at which the exponent α changes its sign. For the O(n) vector model, an estimate based on the fixed $d=3$ six-loop RG expansion reads [15] $n_c=1.945\pm 0.002$. We get for the correlation length critical exponent in the Heisenberg O(2) FP $\nu=0.684$; via the hyperscaling relation this leads to $\alpha=-0.053$. Our estimate correctly reproduces the absence of a divergency in the specific heat of the O(2) model (α is negative); however, the value of $n_c\simeq 1.6$ that we get is rather underestimated. Note, however, that the fixed d approach we exploit in two-loop approximation is essentially better than the corresponding ε expansion. Indeed, in two-loop ε expansion one gets $n_c=4-4\varepsilon$, which does not lead to reasonable estimates [16]. The two-loop estimate of the massive field theory at $d=3$, $n_c\simeq 2.01$ [17], is closer to the most accurate value of Ref. [15], but it gives the wrong sign for the exponent α. In any case the negative value of α for $n=2$ agrees with other calculations as reported in paper I.

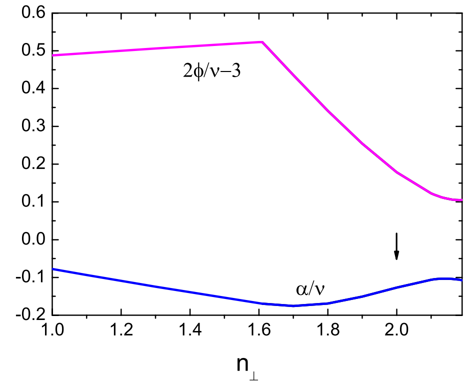

FIG. 1. (Color online) Exponents α/ν and $2\phi/\nu-3$ appearing in Eqs. (72) and (74) at $n_{\parallel}=1$ as functions of $n_{\perp}$. Note that, via relation (105) $2\phi/\nu-3=z-2$, the strong dynamical scaling exponent z results.

It turns out (see below) that case (b) is the stable FP for the asymmetric couplings. In order to evaluate numerically the values of the couplings $\gamma^2_{\parallel}$ and $\gamma^2_{\perp}$, we therefore substitute the resummed fixed point values of the static couplings $\{u_{\parallel},u_{\perp},u_{\times}\}$ into formulas (78) and (79) and resum the resulting expression. In principle, one can use different ways for such an evaluation. Indeed, as we did before, one can present these formulas in the forms of expansions in renormalized couplings (keeping the two-loop terms) and resum the resulting second-order polynomial. Alternatively, based on the observation that the numerator and denominator of Eqs. (78) and (79) contain combinations of critical exponents, one can resum the numerator and the denominator separately. We will exploit both ways, which naturally will lead to slightly different numerical estimates. This difference may also serve to get an idea about the typical numerical accuracy of the results. Separately, we will evaluate the ratios $\gamma_{\perp}/\gamma_{\parallel}$. Again, it will be done by resummation of the series for this ratio, Eq. (73), as well as by using resummed values for $\gamma^2_{\parallel}$ and $\gamma^2_{\perp}$. In particular, for $n_{\parallel}=1$, $n_{\perp}=2$ we get $(\gamma^{\star}_{\perp})^2=0.034$, $(\gamma^{\star}_{\parallel})^2$

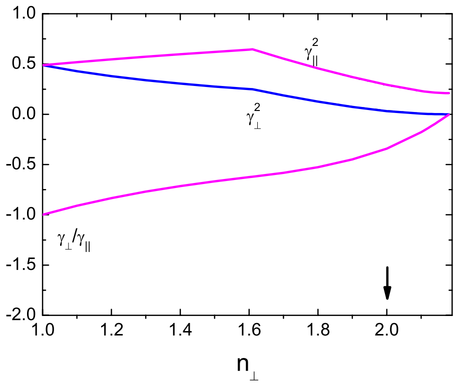

FIG. 2. (Color online) Fixed point values of the asymmetric static couplings $\gamma_\parallel$ and $\gamma_\perp$ for case (b) ($\gamma_\perp^\star=0$, $\gamma_\parallel^\star\neq 0$) at the Heisenberg FP ($n_\perp<1.61$) and the biconical FP ($1.61<n_\perp<2.18$).

$=0.286$ (when the denominator and numerator are resummed separately), and $(\gamma_\perp^\star)^2=0.031$, $(\gamma_\parallel^\star)^2=0.293$ (when an entire expression is resummed). Resulting differences of the order of several percent bring about a typical numerical accuracy of the estimates. In Fig. 2 we plot the FP values of the asymmetric couplings and their ratio obtained within resummation of the entire expressions. These values will be used below to calculate the critical dynamics.

B. Static transient exponents

The stability of the fixed points is determined by the sign of the corresponding transient exponents. The latter can be found from the eigenvalues of the matrix

$$\frac{\partial \beta_{\gamma_\alpha}}{\partial \gamma_\beta} \tag{88}$$

with $\alpha,\beta=\perp,\parallel$. Inserting (43) into (88), the corresponding eigenvalues read

$$\lambda^{(\pm)}=\frac{1}{2}\Bigg\{-\varepsilon+n_\perp\gamma_\perp^2+n_\parallel\gamma_\parallel^2+[\zeta_{\phi^2}]_{11}+[\zeta_{\phi^2}]_{22}\pm\Bigg[\left(\frac{n_\perp\gamma_\perp^2-n_\parallel\gamma_\parallel^2}{2}+[\zeta_{\phi^2}]_{11}-[\zeta_{\phi^2}]_{22}\right)^2+(n_\perp\gamma_\perp\gamma_\parallel+2[\zeta_{\phi^2}]_{12})(n_\parallel\gamma_\perp\gamma_\parallel+2[\zeta_{\phi^2}]_{21})\Bigg]^{1/2}\Bigg\}. \tag{89}$$

The above eigenvalues are valid in two-loop order because Eq. (75) has already been used. The transient exponents

$$\omega_\gamma^{(\pm)}\equiv\lambda^{(\pm)}(\{u\}=\{u^\star\},\{\gamma\}=\{\gamma^\star\}) \tag{90}$$

are calculated by inserting the fixed point values of the static couplings into the eigenvalues. With the fixed point values (82)–(84) and Eq. (89), we obtain for the isotropic Heisenberg FP the following transient exponents.

Case (a): $\gamma_+^\star\neq 0$, $\gamma_-^\star=0$:

$$\omega^{(+)}=\frac{\alpha}{\nu},\quad \omega^{(-)}=-\bar{W}^\star. \tag{91}$$

Case (b): $\gamma_+^\star=0$, $\gamma_-^\star\neq 0$:

$$\omega^{(+)}=2\frac{\phi}{\nu}-d,\quad \omega^{(-)}=\bar{W}^\star. \tag{92}$$

$\bar{W}^\star$ is the root

$$\bar{W}\equiv\sqrt{([\zeta_{\phi^2}]_{11}-[\zeta_{\phi^2}]_{22})^2+4[\zeta_{\phi^2}]_{12}[\zeta_{\phi^2}]_{21}} \tag{93}$$

taken at the fixed point values of the couplings. It is always positive and at the isotropic Heisenberg FP in two-loop order is given by

$$\bar{W}^\star=\frac{n_\perp+n_\parallel}{6}u^\star\left(1-\frac{u^\star}{3}\right). \tag{94}$$

Thus one concludes that case (b) is the stable FP even if α is positive [19]. For the biconical FP the stability of case (b) can be verified explicitly by the flow of the couplings.

C. Dynamical fixed points

Calculations of the dynamical FP values are done by solving the FP equations for the dynamical β functions. Since only two of the equations (53)–(55) are independent, the third equation serves as a consistency check of the solution found. It is useful to choose for this purpose Eqs. (54) and (55) for the time scale ratios $w_\parallel$ and $w_\perp$. Then one has to solve

$$\beta_{w_\parallel}(w_\parallel,w_\perp,w_\parallel/w_\perp)=0,$$

$$\beta_{w_\perp}(w_\parallel,w_\perp,w_\parallel/w_\perp)=0. \tag{95}$$

To find the dynamical FP values, the resummed FP values of the static couplings $u_\parallel^*$, $u_\perp^*$, $u_\times^*$, $\gamma_\perp^*$, and $\gamma_\parallel^*$ are inserted into these equations [18].

The dynamical FPs depend on which static FP is considered. There might be several dynamical FPs for one static FP,

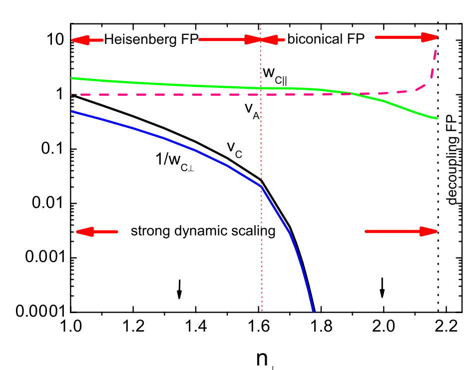

FIG. 3. (Color online) Fixed point values of the time scale ratios v, $1/w_\perp$, and $w_\parallel$ for the static stable FPs: the isotropic Heisenberg FP ($n_\perp<1.61$) and the biconical FP ($1.61<n_\perp<2.18$). Strong dynamical scaling is valid up to the stability borderline to the decoupling FP. In the biconical region the values of v_C and $1/w_{C\perp}$ are finite but cannot be distinguished from zero on this scale. The notation for the dynamical FPs corresponds to the notation in Table II. The dashed curve shows the unstable model A FP (see text).

TABLE II. Types of dynamical FPs for the static Heisenberg and biconical FPs. Not included is the trivial unstable fixed point with all time scale ratios equal to zero. The value of c reads $c=6\ln(4/3)-1$. Note that for the weak scaling FP the result is valid only in two-loop order, whereas the relation of the dynamical critical exponent in the strong scaling FP holds in all orders.

FP	Scaling type	v	$w_\parallel$	$w_\perp = w_\parallel / v$	$z_{\phi_\parallel}$	$z_{\phi_\perp}$	z_m
$\mathcal{H}_{C_w}$	Weak	0	$w^{\mathcal{H}}_{\parallel C_w}$	∞	$2(\phi/\nu)-1$	Infinitely fast	$2(\phi/\nu)-1$
$\mathcal{H}_A$	Weak	$v_A^{(\mathcal{H})}$	0	0	$2+c\eta$	$2+c\eta$	$2(\phi/\nu)-1$
$\mathcal{H}_C$	Strong	$v_C^{\mathcal{H}}$	$w_\parallel^{\mathcal{H}}$	$w_\perp^{\mathcal{H}}$	$2(\phi/\nu)-1$	$2(\phi/\nu)-1$	$2(\phi/\nu)-1$
$\mathcal{B}_{C_w}$	Weak	0	$w^{\mathcal{B}}_{\parallel C_w}$	∞	$2(\phi/\nu)-1$	Infinitely fast	$2(\phi/\nu)-1$
$\mathcal{B}_A$	Weak	$v_A^{(\mathcal{B})}$	0	0	$z^{\mathcal{B}}$	$z^{\mathcal{B}}$	$2(\phi/\nu)-1$
$\mathcal{B}_C$	Strong	$v_C^{(\mathcal{B})}$	$w_\parallel^{\mathcal{B}}$	$w_\perp^{\mathcal{B}}$	$2(\phi/\nu)-1$	$2(\phi/\nu)-1$	$2(\phi/\nu)-1$

which could be either strong or weak dynamical scaling FPs. Since also unstable static FPs might be reached in the asymptotics if one starts with static initial conditions in the attraction region of this FP (a subspace in the space of the static couplings; see, e.g., Fig. 3 in paper I) at least both the Heisenberg FP and the biconical FP have to be taken into consideration. It turns out that in both cases, apart from the trivial unstable FP where all time scale ratios are zero (see below), two dynamical FPs are found: (i) an unstable weak dynamical scaling FP corresponding to model A and (ii) a stable new strong dynamical scaling FP. In the physically interesting case $n_\parallel=1$ and $n_\perp=2$, these cases correspond to dynamical behavior at a multicritical point of bicritical and tetracritical type, respectively. The different types of weak and strong dynamical FPs are shown in Table II.

1. Strong dynamical scaling fixed point

In order to find the strong dynamical scaling FPs it is not necessary to discriminate between the static Heisenberg FP and the biconical FP, although the dynamical equations to be solved are slightly simplified in the first case. Thus we use the results for the FP values derived in paper I for the quartic couplings $\{u\}$ and the FP values for the asymmetric couplings $\{\gamma\}$ of case (b) [see Eqs. (73), (78), and (79)]. At the strong scaling dynamical FP, all time scale ratios have to be nonzero and finite. Moreover, due to the definitions of the time scale ratios, it follows that $w_\parallel^\star = v^\star w_\perp^\star$. This dynamical strong scaling FP value is found by setting the differences of two of the three dynamical ζ functions (44)–(47) to zero, leading to three equations. Since there are only two independent time ratios, the third equation can be used to check the results.

The FP values (FP with subscript C in Table II) have been plotted in Fig. 3 for different $n_\perp$ at $n_\parallel=1$ and the numerical values for $n_\perp=2$ are collected in Table III. This shows that the FP value of the time scale ratio for v is different from the FP value found in the pure relaxational model A. These were at the Heisenberg FP $v_A^\star=1$ and at the biconical FP $v^\star=v_A^{\mathcal{B}}$ with $v_A^{\mathcal{B}}\to\infty$ in approaching the stability borderline to the decoupling fixed point (see Fig. 1 in paper II).

A numerical problem arises in finding the FP values of v and $1/w_\perp$ when they reach very small values. It cannot be decided numerically whether the FP values are zero or finite. In order to clarify the existence or nonexistence of a weak scaling FP, one has to look for an analytic expression for the small FP values. However, it is numerically easy to find a FP value of $w_\parallel$ that is nonzero and finite in the whole region up to the stability borderline between the biconical and decoupling FPs. In order to solve this problem the dependence of the ζ functions are studied within this region. One observes that there are logarithmic terms which would diverge in the limit $v\to 0$ under the condition $w_\perp = w_\parallel / v$. Thus one obtains two equations for the FP values of v and $w_\parallel$. In the equation for the FP of $w_\parallel$ one might safely perform the limit $v\to 0$ and $w_\perp\to\infty$. This leads to

$$0=\zeta_{\Gamma_\parallel}^{(C)}(\{u^\star\},\{\gamma^\star\},v=0,w_\parallel,w_\perp\to\infty)-2\zeta_m^\star. \tag{96}$$

Using the limiting functions

$$\zeta_{\Gamma_\parallel}^{(A)}=\frac{n_\parallel+2}{36}u_\parallel^{\star 2}\left(3\ln\frac{4}{3}-\frac{1}{2}\right)-\frac{n_\perp}{72}u_\times^{\star 2} \tag{97}$$

and

TABLE III. FP values of couplings and time scale ratios for $n_\parallel=1$, $n_\perp=2$.

FP	$u_\parallel^\star$	$u_\perp^\star$	$u_\times^\star$	$\gamma_\parallel^{\star 2}$	$\gamma_\perp^{\star 2}$	$v^\star$	$w_\perp^\star$	$w_\parallel^\star$
$\mathcal{B}_C$ [a]	1.28745	1.12769	0.30129	0.29378	0.03170	6.09592×10^{-43}	1.24285×10^{42}	0.75763
$\mathcal{H}_C$ [b]	1.00156	1.00156	1.00156	0.72554	0.18139	7.29393×10^{-5}	1.55665×10^{4}	1.13541
$\mathcal{H}_C$ [a]	1.00156	1.00156	1.00156	0.72554	0.18139	7.30771×10^{-5}	1.55372×10^{4}	1.13541

[a]FP values of the time scale ratios found via approximation using Eqs. (100) and (101), as described in the text with the values for FP $\mathcal{B}$ of $A=0.097\,70$, $B=0.001\,01$ and for the FP $\mathcal{H}$ of $A=0.315\,34$, $B=0.033\,11$.
[b]Numerical solution for the FP values of the time scale ratios.

$$\bar{\zeta}_{\Gamma_\parallel}^{(C_\parallel)}(u_\parallel^\star,\gamma_\parallel^\star,w_\parallel)=\frac{w_\parallel\gamma_\parallel^{\star 2}}{1+w_\parallel}\Bigg\{1-\frac{1}{2}\Bigg[\frac{n_\parallel+2}{3}u_\parallel^\star\left(1-3\ln\frac{4}{3}\right)+\frac{w_\parallel\gamma_\parallel^{\star 2}}{1+w_\parallel}\left(\frac{n_\parallel}{2}-\frac{w_\parallel}{1+w_|}-\frac{3(n_\parallel+2)}{2}\ln\frac{4}{3}-\frac{(1+2w_\parallel)}{1+w_\parallel}\ln\frac{(1+w_\parallel)^2}{1+2w_\parallel}\right)\Bigg]\Bigg\}, \tag{98}$$

then Eq. (96) reads

$$0=\frac{w_\parallel\gamma_\parallel^{\star 2}}{1+w_\parallel}\Bigg\{1-\frac{1}{2}\Bigg[\frac{n_\parallel+2}{3}u_\parallel^\star\left(1-3\ln\frac{4}{3}\right)+\frac{w_\parallel\gamma_\parallel^{\star 2}}{1+w_\parallel}\left(\frac{n_\parallel}{2}-\frac{w_\parallel}{1+w_\parallel}-\frac{3(n_\parallel+2)}{2}\ln\frac{4}{3}-\frac{1+2w_\parallel}{1+w_\parallel}\ln\frac{(1+w_\parallel)^2}{1+2w_\parallel}\right)\Bigg]\Bigg\}-\frac{n_\perp}{4}\frac{w_\parallel\gamma_\parallel^\star\gamma_\perp^\star}{1+w_\parallel}\left(\frac{2}{3}u_\times+\frac{w_\parallel\gamma_\parallel^\star\gamma_\perp^\star}{1+w_\parallel}\right)+\frac{n_\parallel+2}{36}u_\parallel^{\star 2}\left(3\ln\frac{4}{3}-\frac{1}{2}\right)-\frac{n_\perp}{72}u_\times^{\star 2}-2\zeta_m^\star. \tag{99}$$

This equation is solved numerically to give the value of $w_\parallel^\star$ which then is inserted into the second equation for $v^\star$. In order to find $v^\star$ one collects the logarithmically diverging terms in the equation for $v^\star$,

$$\zeta_{\Gamma_\parallel}^{(C)}(v,w_\parallel,w_\parallel/v)-\zeta_{\Gamma_\perp}^{(C)}(v,w_\parallel,w_\parallel/v)=0. \tag{100}$$

In the remaining terms the limit $v\to 0$ can be safely performed. Then the solution reads

$$\ln v^\star=-\frac{A}{B} \tag{101}$$

with

$$A=2\zeta_m^\star-\gamma_\perp^{\star 2}\Bigg\{1-\frac{1}{2}\Bigg[\frac{n_\perp+2}{3}u_\perp^\star\left(1-3\ln\frac{4}{3}\right)+\gamma_\perp^{\star 2}\left(\frac{n_\perp}{2}-1-\frac{3(n_\perp+2)}{2}\ln\frac{4}{3}-2\ln\frac{w_\parallel^\star}{2}\right)\Bigg]\Bigg\}+\frac{n_\parallel}{4}\gamma_\perp^\star\gamma_\parallel^\star\left(\frac{2}{3}u_\times^\star+\gamma_\perp^\star\gamma_\parallel^\star\right)\ln 2-\frac{n_\perp+2}{36}u_\perp^{\star 2}\left(3\ln\frac{4}{3}-\frac{1}{2}\right)-\frac{n_\parallel}{72}u_\times^{\star 2}(1-2\ln 2) \tag{102}$$

and

$$B=\gamma_\perp^{\star 4}+\frac{n_\parallel}{36}u_\times^{\star 2}+\frac{n_\parallel}{4}\gamma_\perp^\star\gamma_\parallel^\star\left(\frac{2}{3}u_\times^\star+\gamma_\perp^\star\gamma_\parallel^\star\right). \tag{103}$$

It can be shown that A and B are positive. On approach to the stability borderline to the decoupling FP, A stays finite and B goes to zero since $u_\times^\star$ and $\gamma_\perp^\star$ go to zero. In consequence $v^\star$ goes to zero and $w_\perp^\star$ goes to infinity in and only in this limit. The analytic solution found within this region joins smoothly to the numerical solution found for larger values of the time scale ratios. Thus it is proven that in the whole region where the Heisenberg FP or the biconical FP is stable dynamical strong scaling holds.

Considering the FP values for the time scale ratios for the Heisenberg FP in the region of $n_\perp>1.7$ (where it is reached only for static initial conditions in a subspace of the fourth-order couplings) one also finds a small value for $v^\star$, a very large value for $w_\perp^\star$, and a nonzero finite value for $w_\parallel^\star$. However, contrary to the biconical FP now A and B stay finite at the stability borderline between the biconical FP and the decoupling FP at $n_\perp\sim 2.18$. Indeed, the values calculated for the Heisenberg FP from Eqs. (102) and (103) are $A=0.348\,66$, $B=0.025\,58$, whereas for the biconical FP one obtains $A=0.052\,68$, $B=4.279\,58\times 10^{-9}$.

The asymptotic dynamical exponents are obtained from the values of the ζ functions at the FP:

$$z_{\phi_\parallel}=2+\zeta_{\Gamma_\parallel}^\star,\quad z_{\phi_\perp}=2+\zeta_{\Gamma_\perp}^\star,\quad z_m^\star=2+\zeta_\lambda. \tag{104}$$

At the strong dynamical scaling FP all dynamical ζ functions are equal to twice the static ζ function ζ_m. Therefore the CD induces the value of the dynamical critical exponent z

$$z=2+2\zeta_m^\star=2\frac{\phi}{\nu}-1 \tag{105}$$

according to Eqs. (39) and (74). The values for the static exponents depend on which static FP is stable. For $n_\parallel=1$ the $n_\perp$ dependence of $z-2$ is shown in Fig. 1.

2. Weak dynamical scaling fixed point

Weak dynamical scaling FPs are solutions of the dynamical FP equations where one or more of the FP values of the time scale ratios are zero or infinite. Such a weak dynamical scaling FP has already been found in model A and it became stable at the stability borderline to the decoupling FP.

Indeed, Eqs. (95) allow solutions where both time scale ratios $w_\parallel$ and $w_\perp$ are zero. In such a case one has to rely on the third equation for the ratio $v=w_\parallel/w_\perp$ to find the limiting FP value. However, in the limit $w_\parallel\to 0$ and $w_\perp\to 0$ Eq. (53) for v reduces to the FP equation of model A (FP with subscript A in Table II). Thus one recovers the model A FPs in this case.

There is no solution $w_\parallel^\star=v^\star=0$ and $w_\perp$ nonzero and finite due to the $\ln v$ term in (50). For a similar reason, no FP with $w_\parallel^\star$ nonzero and finite, $w_\perp^\star=0$, and $v^\star=\infty$ is possible. However, a FP with $w_\parallel^\star$ nonzero and finite, $v^\star=0$, and $w_\perp=\infty$ is possible (FP with subscript C_w in Table II). The values of $w_\parallel^\star$ are obtained from Eq. (99), but now these values are not an approximation but the exact C_w FP values for any $n_\parallel$ and $n_\perp$.

The dynamical critical exponents may be different in the case of weak dynamical scaling. For the weak model C FP (subscript Cw) $w_\parallel^\star$ is finite and nonzero, therefore $\zeta_{\Gamma_\parallel}^\star=\zeta_\lambda^\star$ and $z_{\phi_\parallel}=2(\phi/\nu)-1$. Thus the CD sets the time scale for the OP $\phi_\parallel$. Inserting $w_\perp^\star=\infty$ into $\zeta_{\Gamma_\perp}$ leads due to logarithmically diverging terms to an infinite value of the corresponding dynamical exponent $z_{\phi_\perp}$. This indicates that the density $\phi_\perp$ is much faster than the other densities. It is especially much faster than the other OP $\phi_\parallel$.

In the case where both FP values of the time scale ratios $w_\parallel$ and $w_\perp$ are zero and v is finite and nonzero, both OPs have the same time scale with the dynamical exponent (of model A) $z=2+c\eta$, different from the exponent of the CD, $z_m=2\phi/\nu-1$.

D. Dynamical transient exponents

The dynamical transient exponents can be calculated from the matrix of the derivatives of the β function with respect to the time scale ratios v, $w_\parallel$, and $w_\perp$. Since only two time scale ratios are independent, only two are considered in the stability matrix. The eigenvalues of the 2×2 matrix have to be positive for an overall stable FP, otherwise the FP is unstable. In the following the time scale ratios $w_\parallel$ and $w_\perp$ are chosen as independent.

The model A type FP with $v^\star=v_A$ nonzero and finite is unstable since the two eigenvalues

$$\omega_{w_\parallel}=\zeta^\star_{\Gamma_\parallel}-2\zeta^\star_m \quad \text{and} \quad \omega_{w_\perp}=\zeta^\star_{\Gamma_\perp}-2\zeta^\star_m \tag{106}$$

are negative. In fact they are equal, because $\zeta^\star_{\Gamma_\parallel}=\zeta^\star_{\Gamma_\perp}$. Their values are calculated with $2\zeta^\star_m=2\phi/\nu-1$ and inserting the model A FP value $v^\star=v_A$ (see Fig. 3) and $w^\star_\parallel=w^\star_\perp=0$. Then $\zeta^\star_{\Gamma_\parallel}-2\phi/\nu+1<0$ and $\omega_{w_\parallel}=-0.126$ for $n_\parallel=1$ and 2.

Similarly, the instability of the FP with $v^\star=w^\star_\parallel=w^\star_\perp=0$ can be shown. However, some care has to be taken due to the vanishing time scale ratio v. The eigenvalues are again given by Eq. (106) but now they are different. Whereas $\omega_{w_\parallel}$ is negative, $\omega_{w_\perp}$ goes to ∞ due to the $\ln v$ term in the model A ζ function (50).

The transient exponents for the strong scaling FPs are the eigenvalues of the matrix of derivatives of the β functions according to the time scale ratios at the FP,

$$\begin{pmatrix} \frac{\partial\beta_{w_\parallel}}{\partial w_\parallel} & \frac{\partial\beta_{w_\parallel}}{\partial w_\perp} \\ \frac{\partial\beta_{w_\perp}}{\partial w_\parallel} & \frac{\partial\beta_{w_\perp}}{\partial w_\perp} \end{pmatrix}^\star = \begin{pmatrix} w_\parallel\left(\frac{\partial\zeta_{\Gamma_\parallel}}{\partial w_\parallel}\right) & w_\parallel\left(\frac{\partial\zeta_{\Gamma_\parallel}}{\partial w_\perp}\right) \\ w_\perp\left(\frac{\partial\zeta_{\Gamma_\perp}}{\partial w_\parallel}\right) & w_\perp\left(\frac{\partial\zeta_{\Gamma_\perp}}{\partial w_\perp}\right) \end{pmatrix}^\star . \tag{107}$$

Use has been made of the lack of dependence of ζ_λ on the time scale ratios. The nondiagonal elements depend on the time scale ratios by which they are derived only via v and therefore are proportional to $1/w_\perp$. In the region where $w_\perp$ is very large, the two eigenvalues are then given by the diagonal elements

$$\omega_{w\parallel}=w^\star_\parallel\left(\frac{\partial\zeta_{\Gamma_\parallel}}{\partial w_\parallel}\right)^\star, \quad \omega_{w_\perp}=w^\star_\perp\left(\frac{\partial\zeta_{\Gamma_\perp}}{\partial w_\perp}\right)^\star. \tag{108}$$

Near the stability borderline to the decoupling FP, the second eigenvalue goes to zero according to

$$\omega_{w_\perp}=B+O(1/w_\perp) \tag{109}$$

with B from Eq. (103), being exactly zero at the borderline. The value of the slow transient at $n_\parallel=1$ and $n_\perp=2$ is given by $\omega_{w_\perp}=0.001$. Thus, as shown in the next section, in this case nonasymptotic effects are present in the physically accessible region.

As already mentioned for the Heisenberg FP $\mathcal{H}_C$, B does not reach zero at the borderline but its value is one order smaller than the static transient exponents. At $n_\perp=2$ and 2.18 the value of the dynamical transient exponent is given by $\omega_{w_\perp}=0.033$ and 0.026, respectively.

VI. DYNAMICAL FLOWS AND EFFECTIVE EXPONENTS

The flow of the time scale ratios is described by the RG equations

$$l\frac{\partial v}{\partial l}=\beta_v(\{u\},\{\gamma\},\{w\}),$$

$$l\frac{\partial w_\perp}{\partial l}=\beta_{w_\perp}(\{u\},\{\gamma\},\{w\}),$$

$$l\frac{\partial w_\parallel}{\partial l}=\beta_{w_\parallel}(\{u\},\{\gamma\},\{w\}), \tag{110}$$

with the β functions Eqs. (53) and (54). Note that the dynamical β functions depend also on the RG equations of the static quartic couplings [Eqs. (33)–(36) of paper I] and the RG equations of the asymmetric couplings,

$$l\frac{\partial\vec{\gamma}}{\partial l}=\vec{\beta}_\gamma(\{u\},\{\gamma\}), \tag{111}$$

with the β function Eq. (43).

In order to simplify the picture, it is assumed that the static couplings have already reached the FP by which they are attracted from their initial conditions. Then the RG flows are displayed in the three-dimensional space of the time scale ratios $w_\parallel$, $w_\perp$, v in Figs. 4 and 5 for the physically interesting case at $n_\parallel=1$, $n_\perp=2$. The static biconical FP is stable for this case in general. However, for initial conditions on the surface separating the stable biconical FP from the Heisenberg FP the flow is attracted to the Heisenberg FP. Therefore one may also fix the static parameters to this FP.

To give an overview of the different patterns of the flows three different value of $n_\perp$ are chosen for fixed $n_\parallel=1$: (i) $n_\perp=1.2$, where the static Heisenberg FP is stable (Fig. 4(a)), (ii) $n_\perp=1.7$ (Fig. 4(b)), and (iii) $n_\perp=2$ (Fig. 5), where the biconical FP is stable.

In all cases the FP values of the time scales are nonzero and finite but the values of $v^\star$ becomes very small and $w^\star_\perp$ very large. The asymptotic approach to the FP in cases (ii) and (iii) occurs in the direction of the $w_\perp$ axis almost at $v\sim 0$ and $w_\parallel\sim w^\star_\parallel$.

Effective exponents

We define the effective exponents by:

$$z_{\parallel\text{eff}}(l)=2+\zeta_{\Gamma_\parallel}(\{u(l)\},\{\gamma(l)\},\{w(l)\}),$$

$$z_{\perp\text{eff}}(l)=2+\zeta_{\Gamma_\perp}(\{u(l)\},\{\gamma(l)\},\{w(l)\}),$$

$$z_{m\ \text{eff}}(l)=2+\zeta_\lambda(\{u(l)\}). \tag{112}$$

These exponents appear, e.g., in the critical temperature and/or wave vector dependence of the transport coefficients

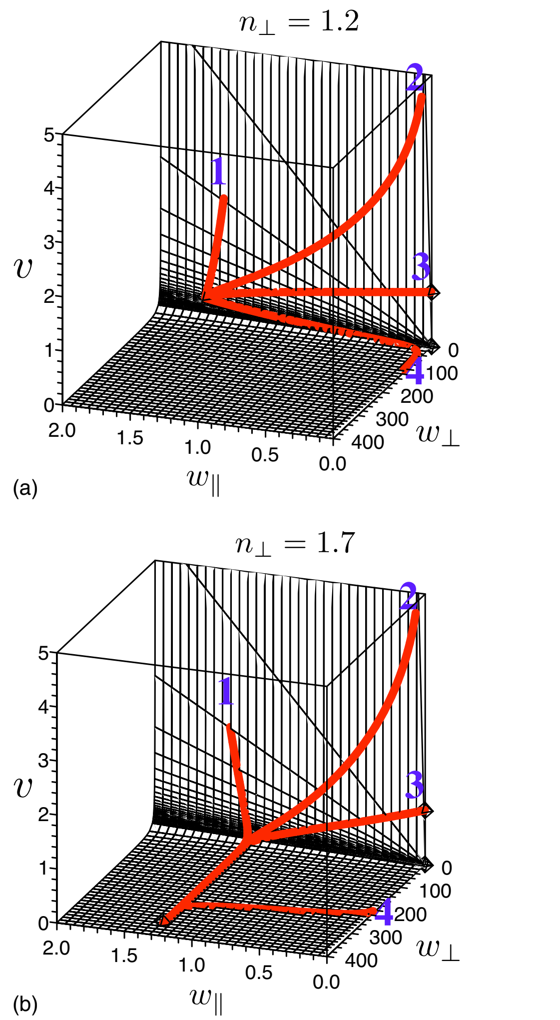

FIG. 4. (Color online) Dynamical flow at $n_\parallel=1$ and different $n_\perp$ values for different dynamical initial conditions numbered 1 to 4. The static couplings are chosen to be fixed at their stable FP values (the isotropic Heisenberg FP for $n_\perp=1.2$, the biconical FP for $n_\perp=1.7$). The dynamical FP values are $v^\star=0.399$ (0.004), $w_\parallel^\star=1.661$ (1.300), and $w_\perp^\star=4.159$ (351.06) at $\mathcal{H}_C$ ($\mathcal{B}_C$), respectively. Also shown is the surface $v=w_\parallel/w_\perp$ to which the flow is restricted.

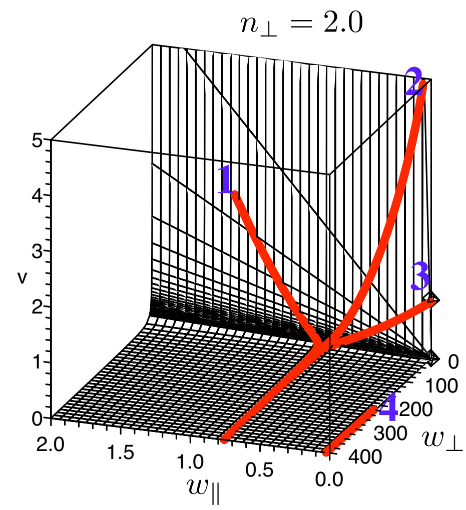

FIG. 5. (Color online) Dynamical flow at $n_\parallel=1$ and $n_\perp=2$ for different dynamical initial conditions numbered 1 to 4. The static couplings are chosen to be fixed at their biconical FP values. The static and dynamical FP values of $\mathcal{B}_C$ are given in Table III. The dynamical FP lies outside the region shown. Also shown is the surface $v=w_\parallel/w_\perp$ to which the flow is restricted.

describing the relaxation of the alternating magnetization or the diffusion of the magnetization in the direction of the external magnetic field. They are in principle experimentally accessible. An interesting feature is the lack of dependence of the effective dynamical scaling exponent z_m of the CD on the dynamical time scales. Therefore its nonasymptotic value is due only to nonasymptotic effects within statics. This allows us to trace back nonasymptotic effects in dynamical quantities to the slow transients in statics or those appearing in the dynamics.

In order to calculate the numerical values of the effective exponents, we substitute into Eq. (112) the resummed coordinates of the static FP $\{u_\parallel^*, u_\perp^*, u_\times^*\}$ and the values of time scale ratios $\{w_\parallel(l), w_\perp(l), v(l)\}$ along the RG flow. Choosing the FP values of the static couplings fixes the asymptotic values of the effective dynamical exponents since they are expressed by the static asymptotic exponents for the strong dynamical scaling FP.

The results shown in Fig. 6 correspond to the case $n_\parallel=1$, $n_\perp=2$. We evaluate the time scale ratios along the previously obtained flows 1–4 in Fig. 5. The effective exponents for the different initial conditions are shown by numbered solid lines. As one can observe from this figure, the exponents calculated along several flows do not coincide for the values of the flow parameter shown. However, one sees the merging of the different values for $z_\parallel$ to their asymptotic value $z_\perp^\star = z_m^\star = 2.18$ given by the static value corresponding to the CD (the constant line in Fig. 6). More remarkable is the difference between the effective exponents for the parallel and perpendicular components of the OP. This difference can

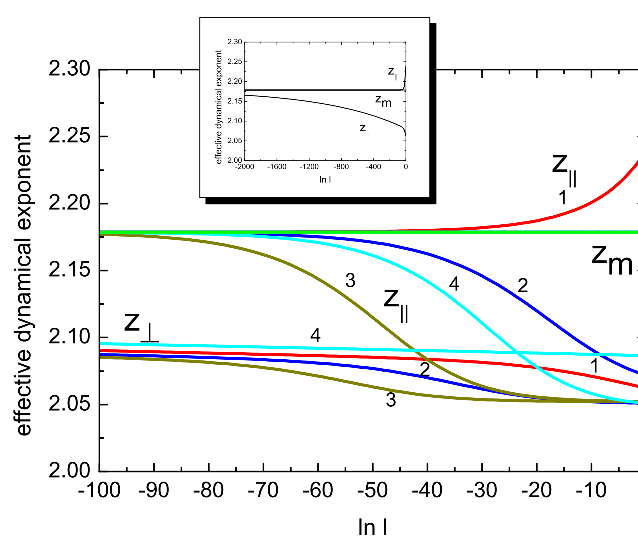

FIG. 6. (Color online) Effective dynamical exponents $z_\parallel$, $z_\perp$, and z_m calculated along the different RG flows of Fig. 5 (indicated by the numbers). The inset shows that even for flow parameters as small as $\ln l = -2000$ the effective exponent $z_\perp$ has not reached its asymptotic value 2.18.

be traced back to the fact that $w_\perp$ did not reach its very large FP value due to the slow dynamical transient. Only for flow parameter values larger than $\ln l \sim -2000$ does the effective exponent attain its asymptotic value $z_\perp \sim 2.18$ as it should (see the inset of Fig. 6 where the smallest value is $\ln l = -2000$ for the flow 1).

Furthermore, we see that the exponent $z_\parallel$ flows toward its asymptotic value $z_\parallel = 2.18$. In fact, exponent $z_\perp$ attains the asymptotic value $z_\perp = 2.18$ as well, but for much smaller values of the flow parameter. In the inset of Fig. 6 we show this exponent for all flows within a larger range of $\ln l$.

For certain initial values of the *static* parameters it is possible that the unstable Heisenberg FP is reached (see Fig. 3 in paper I for the flow number 1) for the flow number 1, which lies on the surface separating the attraction region of the biconical FP from the runaway solutions. In such a case the effective exponents reach the asymptotic value of the dynamical exponent $z = 2.44$ more quickly since the dynamical transient exponent $\omega_{w_\perp} = B$ is larger by a factor of 33 (for the values of B see footnotes to Table III).

VII. CONCLUSION AND OUTLOOK

The effect of coupling the conserved magnetization parallel to the external magnetic field to the two OPs (the components of the alternating magnetization parallel and perpendicular to the external magnetic field) leads to strong scaling dynamical behavior. This means that the time scales of all dynamical quantities scale with the same dynamical critical exponent $z = 2\phi/\nu - 2$. However, this scaling behavior might be hidden by nonasymptotic effects dominating the physically accessible region when approaching the multicritical point due to a very small dynamical transient. This applies in the physically interesting case $n_\parallel = 1$ and $n_\perp = 2$, where one of the time scales is almost zero and the other one almost infinite. In consequence the magnetic transport coefficients might show different effective behavior with temperature when the multicritical point is approached. The dynamical amplitude ratios might be far from their asymptotic values and show nonuniversal behavior.

For a complete description in the whole $n_\parallel - n_\perp$ space, the model presented here has to be extended in two ways. First, for the physical case $n_\parallel = 1$ and $n_\perp = 2$, one has to introduce reversible terms in the equations of motions. Second, one has to allow for an asymmetric coupling to an energylike CD in addition to the magnetization.

ACKNOWLEDGMENT

This work was supported by the Fonds zur Förderung der wissenschaftlichen Forschung under Project No. P19583-N20.

[1] R. Folk, Yu. Holovatch, and G. Moser, Phys. Rev. E **78**, 041124 (2008).

[2] R. Folk, Yu. Holovatch, and G. Moser, Phys. Rev. E **78**, 041125 (2008).

[3] V. Dohm and H.-K. Janssen, Phys. Rev. Lett. **39**, 946 (1977); J. Appl. Phys. **49**, 1347 (1978).

[4] Since at the multicritical point two different types of fluctuation are present corresponding to the two OPs, there are also two types of slow conserved densities: (i) magneticlike and (ii) energylike. They correspond to the two fields: (i) the magnetic field and (ii) the temperature.

[5] V. Dohm, Kernforschungsanlage Jülich Report No. 1578, 1979 (unpublished).

[6] V. Dohm, in *Multicritical Phenomena*, NATO ASI Series B Vol. 106, edited by R. Pynn and A. Skjeltrop (Plenum, New York, 1983), p. 81.

[7] B. I. Halperin, P. C. Hohenberg, and Shang-keng Ma, Phys. Rev. B **10**, 139 (1974); E. Brezin and C. De Dominicis, *ibid.* **12**, 4954 (1975).

[8] R. Folk and G. Moser, Phys. Rev. Lett. **91**, 030601 (2003).

[9] D. R. Nelson, J. M. Kosterlitz, and M. E. Fisher, Phys. Rev. Lett. **33**, 813 (1974); Y. Imry, J. Phys. C **8**, 567 (1975); I. F. Lyuksyutov, V. L. Pokrovskii, and D. E. Khmelnitskii, Sov. Phys. JETP **42**, 923 (1975); V. V. Prudnikov, P. V. Prudnikov, and A. A. Fedorenko, JETP Lett. **68**, 950 (1998); P. Calabrese, A. Pelissetto, and E. Vicari, Phys. Rev. B **67**, 054505 (2003).

[10] V. Dohm, Z. Phys. B: Condens. Matter **60**, 61 (1985); R. Schloms and V. Dohm, Europhys. Lett. **3**, 413 (1987); Nucl. Phys. B **328**, 639 (1989).

[11] R. Folk and G. Moser, J. Phys. A **39**, R207 (2006).

[12] R. Folk and G. Moser, Phys. Rev. E **69**, 036101 (2004).

[13] M-C. Chang and A. Houghton, Phys. Rev. B **21**, 1881 (1980).

[14] We use the Padé-Borel resummation technique, as explained in detail in paper I. For an overview, see, e.g., Yu. Holovatch, V. Blavats'ka, M. Dudka, C. von Ferber, R. Folk, and T. Yavors'kii, Int. J. Mod. Phys. B **16**, 4027 (2002).

[15] C. Bervillier, Phys. Rev. B **34**, 8141 (1986).

[16] For estimates of the marginal dimension n_c, see M. Dudka, Yu. Holovatch, and T. Yavors'kii, Acta Phys. Slov. **52**, 323 (2002).

[17] G. Jug, Phys. Rev. B **27**, 609 (1983).

[18] Two cautions are to be made at this point. First, due to the special structure of the dynamical vertex functions, the dynamical β functions contain only even powers of the couplings $\gamma_\perp$ and $\gamma_\parallel$. Therefore, to define a sign of the coupling, one should use an additional condition, Eq. (73). Second, since the formulas for the dynamical β functions are nonpolynomial, one cannot use familiar resummation techniques for further numerical estimates. However, one improves their convergence in an indirect way, by using there the resummed values for the static couplings.

[19] Note that in Eq. (6) only one CD has been taken into account. In the most general case, and especially when the specific heat is diverging, one should allow for a second CD and four asymmetric couplings.